AFOSR-TR- 90 1261

(2)

DEVELOPMENT OF A HIGH EFFICIENCY Q-SWITCHED GLASS LASER VIA SOL-GEL PROCESSING

GELTECH

SBIR PHASE II FINAL TECHNICAL REPORT
PREPARED FOR
AIR FORCE OFFICE OF SCIENTIFIC RESEARCH
BOLLING AFB DC 20332

UNCLASSIFIED
SECURITY CLASSIFICATION OF THIS PAGE

REPORT DOCUMENTATION PAGE

1a. REPORT SECURITY CLASSIFICATION: UNCLASSIFIED	1b. RESTRICTIVE MARKINGS
2a. SECURITY CLASSIFICATION AUTHORITY	3. DISTRIBUTION / AVAILABILITY OF REPORT
2b. DECLASSIFICATION / DOWNGRADING SCHEDULE	
4. PERFORMING ORGANIZATION REPORT NUMBER(S): Final Technical Report	5. MONITORING ORGANIZATION REPORT NUMBER(S): AFOSR-TR- 91 1
6a. NAME OF PERFORMING ORGANIZATION: GELTECH, Inc. / 6b. OFFICE SYMBOL (If applicable)	7a. NAME OF MONITORING ORGANIZATION: Air Force Office of Scientific Research
6c. ADDRESS (City, State, and ZIP Code): One Progress Blvd., Box 18, Alachua, FL 32615	7b. ADDRESS (City, State, and ZIP Code): Building 410, Bolling AFB, DC 20332-6448
8a. NAME OF FUNDING / SPONSORING ORGANIZATION: AFOSR / 8b. OFFICE SYMBOL (If applicable): NC	9. PROCUREMENT INSTRUMENT IDENTIFICATION NUMBER: F49620-89-C-0006
8c. ADDRESS (City, State, and ZIP Code): Bolling Air Force Base, Bldg. 410, Washington, D.C. 20332-6448	10. SOURCE OF FUNDING NUMBERS: PROGRAM ELEMENT NO. 65502F / PROJECT NO. 3005/A1 / TASK NO. / WORK UNIT ACCESSION NO.

11. TITLE (Include Security Classification)

Development of a High Efficiency Q-Switched Glass Laser via Sol-Gel Processing

12. PERSONAL AUTHOR(S)

Dr. Vinay K. Seth and Dr. Jean-Luc Nogues and William V. Moreshead

13a. TYPE OF REPORT	13b. TIME COVERED	14. DATE OF REPORT (Year, Month, Day)	15. PAGE COUNT
Final Technical	FROM 881001 TO 900930	891030	92

16. SUPPLEMENTARY NOTATION

17. COSATI CODES: FIELD	GROUP	SUB-GROUP

18. SUBJECT TERMS (Continue on reverse if necessary and identify by block number)

Sol-Gel, Neodymium, Laser Glass, Silica, Aluminum, Phosphorus, (ZnO)

19. ABSTRACT (Continue on reverse if necessary and identify by block number)

Neodymium-doped silica glass is the most desirable glass for Q-switched and amplifier applications due to broad transmission range, a low nonlinear refractive index, low CTE, high lasing efficiency at room temperature, possibility of large size media and possible use of sensitizers to increase energy efficiency. However, preparation of such a glass by conventional melting requires very high temperature resulting in deleterious contamination from the melting crucible. Addition of fluxes to lower the melting temperature however degrades the physical and the optical properties of the glass. Sol-gel technology is a novel way of fabricating glass without melting. This process uses silicon alkoxides for making a sol which is cast into a gel. Heat treatment of this gel at high temperatures (still much lower than melting) results in glass. This study explored the fabrication of Nd-doped silica glass by two different sol-gel techniques, namely, mixing and impregnation. The latter process, which requires impregnation of an Nd-containing solution into an ultraporous dehydroxylated silica matrix, was successfully developed. A buffer element, Al, was used to prevent cluster quenching of the fluorescence lifetime of the laser glass. Crack-free monolithic disks of ~3.0 weight % Nd_2O_3 in silica glass (about 12 mm in diameter and 4 mm in thickness), which had fluorescence lifetimes of about 300 μs, were fabricated reproducibly.

20. DISTRIBUTION / AVAILABILITY OF ABSTRACT	21. ABSTRACT SECURITY CLASSIFICATION
☒ UNCLASSIFIED/UNLIMITED ☒ SAME AS RPT ☐ DTIC USERS	Unclassified
22a. NAME OF RESPONSIBLE INDIVIDUAL: Dr Donald Ulrich	22b. TELEPHONE (Include Area Code): 202-767-4960 / 22c. OFFICE SYMBOL: NC

DD FORM 1473, 84 MAR — 83 APR edition may be used until exhausted. All other editions are obsolete.

SECURITY CLASSIFICATION OF THIS PAGE

UNCLASSIFIED

ACKNOWLEDGEMENTS

The encouragement of Dr. D.R. Ulrich is gratefully acknowledged along with the financial support from Strategic Defense Initiative (SDI) and Air Force Office of Scientific Research (AFOSR). The research was sponsored by AFOSR under contract #F49620-89-C-0006. The United States Government is authorized to reproduce and distribute reprints for governmental purposes notwithstanding any copyright notation from here on. The authors would like to thank Dr. J. Daly and Dr. W. Williams of Litton Laser Systems, Apopka, FL, and Dr. T.A. King, University of Manchester, U.K., for measuring the fluorescence spectra and lifetimes. Also, the assistance of Mr. E.J. Jenkins of Microanalytical Laboratories, Gainesville, FL, is acknowledged for carrying out transmission electron microscopy.

EXECUTIVE SUMMARY

Neodymium-doped silica glass is the most desirable glass for Q-switched and amplifier applications due to broad transmission range, a low nonlinear refractive index, low CTE, high lasing efficiency at room temperature, possibility of large size media and possible use of sensitizers to increase energy efficiency.

However, preparation of such a glass by conventional melting requires very high temperature resulting in deleterious contamination from the melting crucible. Addition of fluxes to lower the melting temperature however degrades the physical and the optical properties of the glass.

Sol-gel technology is a novel way of fabricating glass without melting. This process uses silicon alkoxides for making a sol which is cast into a gel. Heat treatment of this gel at high temperatures (still much lower than melting) results in glass.

This study explored the fabrication of Nd-doped silica glass by two different sol-gel techniques, namely, mixing and impregnation. The latter process, which requires impregnation of an Nd-containing solution into an ultraporous dehydroxylated silica matrix, was successfully developed. A buffer element, Al, was used to prevent cluster quenching of the fluorescence lifetime of the laser glass. Crack-free monolithic disks of ~3.0 weight % Nd_2O_3 in silica glass (about 12 mm in diameter and 4 mm in thickness), which had fluorescence lifetimes of about 300 μs, were fabricated reproducibly.

The fabrication of high aspect ratio geometries like rods could not be processed in a crack-free manner. Modifications of the final drying procedure are warranted for their successful development. The issues of selection and concentration optimization of sensitizers and the optical quality of the final glass need to be addressed in greater detail.

Hence, this research has successfully developed a process for the fabrication of Nd-doped silica laser glass which has fluorescence lifetimes of about 300 μs and can be manufactured reproducibly and reliably in crack-free form for small dimension disks.

OBJECTIVES OF THE RESEARCH EFFORT

The specific objectives of the Phase II effort were:

1. Modification of processing parameters and composition for disks and rods co-doped with neodymium and aluminum for optimization of gel quality, fluorescence lifetimes, and other lasing characteristics. The ultimate goal here was to prepare materials with excellent lasing properties that are better than silicate laser glasses currently available commercially, while maintaining thermal and optical characteristics as close to those of pure silica as possible.

2. Modification of processing parameters and composition for disks and rods co-doped with neodymium and phosphorus for optimization of gel quality, fluorescence lifetimes, and other lasing characteristics. The ultimate goal of this objective was to prepare new laser materials having the advantages of both phosphate and silicate glasses.

3. Optimization of the use of sensitizers to increase efficiency. The efficiency and power output of a laser can be increased by adding small amounts of other ions which absorb the pump radiation and efficiently transfer it to the appropriate energy level of the lasing species. A number of various ions have been used as sensitizers with Nd. This phenomenon, however, appears to be influenced by the laser host material. Therefore, it was important to investigate sensitizers in the laser glasses produced by sol-gel processing.

4. Demonstrate the production of doped silica sol-gel monoliths with the optimum concentrations of Nd, Al and/or P and sensitizers determined in objectives one through three. This objective focused on the translation of laboratory experiments to pilot-plant type manufacture, including parameters such as quality assurance, repeatability, and reproducibility during scale-up.

LIST OF PUBLICATIONS RESULTING FROM THIS RESEARCH EFFORT

1. W.V. Moreshead, J.L. Noguès and R.H. Krabill, "Preparation, Processing, and Fluorescence Characteristics of Neodymium-Doped Silica Glass Prepared by the Sol-Gel Process," *J. Non-Cryst. Solids*, **121** 267-272 (1990).

2. V.K. Seth, W.V. Moreshead and J.L. Noguès, "Enhanced Fluorescence Lifetime of Nd/SiO_2 Glass Fabricated via Sol-Gel," manuscript in preparation.

3. A.J. Berry and T.A. King, "Characterization of Doped Sol-Gel Derived Silica Hosts for Use in Tunable Glass Lasers," *J. Phys. D: Appl. Phys.*, **22** 1419-1422 (1989).

4. A.J. Berry and T.A. King, "Development of Tunable Doped Gel-Silica Glass Lasers," Presented at *U.S.-U.K. Optical Glass and Macromolecular Materials Symposium #1*, June 14-17, 1988, Pitlochry, U.K.

5. J.L. Noguès and W.V. Moreshead, "Porous Gel-Silica, A Matrix for Optically Active Components," *J. Non-Cryst. Solids*, **121** 136-142 (1990).

6. D. Shaw, C. Whitehurst, A. Charlton and T.A. King, "Tunable Solid State Glass Lasers," Presented at *U.S.-U.K. Optical Glass and Macromolecular Materials Symposium #3*, September 4-7, 1990, Cumbria, U.K.

A copy of these publications are given in Appendices A to F.

LIST OF PROFESSIONAL PERSONNEL ASSOCIATED WITH THE RESEARCH EFFORT

Technical Staff

Jean-Luc R. Noguès - Principal Investigator and Vice President R&D
William V. Moreshead - Research Scientist
Vinay K. Seth - Research Scientist
Bing-Fu Zhu - Research Scientist
Fred Chapman - Group Support Engineer
Steve Black - Technician
Letha Rice - Technical Writer

Corporate Staff

Anthony J. LaPaglia - President & CEO (Present)
James G. Hermann - President & CEO (Former)
Dennis A. LeSage - General Manager (Former)
Joseph L. Lombardi - Secretary and Controller

LIST OF TABLES

LIST OF FIGURES

LIST OF APPENDICES

CONTENTS

RESEARCH REPORT

1 INTRODUCTION

1.1 Property Requirements for Solid-State Laser Materials

A solid-state laser material must absorb pump light which is converted to laser radiation. The absorption and conversion efficiencies must be as high as possible. The amplification (gain), **g**, is given by [1]:

$$\mathbf{g} = \sigma N$$

where,

σ = induced emission cross-section

N = number of active ions per cm^3 of medium

Also, the fluorescence lifetime, τ, should be high so as to use the pumping source more energy-efficiently [1,2]. The nonlinear refractive index, n_2, should be low, especially for high-power lasers where the self-focusing of the beam is critical [1,2]. At the lasing wavelength, the material should have minimum optical loss that is not affected by pump radiation. A high optical homogeneity and low beam distortion due to temperature gradient are desirable. For the latter, the laser must have good thermal shock resistance, especially if the pulse repetition rate is high. Hence, the coefficient given by [1]:

$$s(1-\mu)/\alpha E$$

where,

s = mechanical strength of the medium

μ = Poisson ratio of the medium

α = coefficient of thermal expansion of the medium

E = Young's modulus of the medium

must be high. This glass must also have a high damage threshold, especially for high-power lasers [1,2,3].

1.2 Glasses as Host-Matrices for Laser-Active Ions

Glasses, as laser host materials, have a number of advantages over crystalline materials. The ability to fabricate large size and desired shapes are primary merits along with optical quality (high homogeneity) which is generally excellent. The index of refraction of the host matrix glass can be tailored with relative ease [2]. Also, the ability to control the temperature coefficient of the index of refraction and strain-optic coefficient permits a thermally stable cavity. Also, the use of sensitizers enhances the laser efficiency [1,2,3].

Glasses produced by conventional melting however have low thermal conductivity which limits the diameter of the rod for continuous wave (CW) and high pulse repetition rate applications. Also, the lines obtained are inhomogeneously broadened and wider than those in crystal matrices [2] as depicted in Figure 1. As a result, threshold is difficult to obtain as a larger inversion is required to achieve the same gain at the center of the line. However, it should be noted that a broadened fluorescent line is an advantage for Q-switched and amplifier applications [3]. The broadened line results in lower loss due to amplified spontaneous emission for the same inversion.

As is clear from the above discussion glasses are suitable for high-energy pulsed operations, as opposed to crystals which, due to their higher thermal conductivity and narrower emission linewidths, are suitable for applications that require continuous-wave and high pulse repetition rates [1,2,3].

The most desirable glass for use as a matrix in high-powered lasers is silica glass, since it has a broad transmission range from ultraviolet to infrared, a low nonlinear refractive index, and a very low coefficient of thermal expansion [3]. Neodymium (Nd) doped glass matrix lasers show the greatest promise for high-powered, pulsed-laser applications [2,4]. Neodymium is more favorable to use than the other rare earth ions which have been made to lase in a glass matrix because Nd can be made to lase at room temperatures with comparatively high efficiency. The addition of Nd to a glass matrix

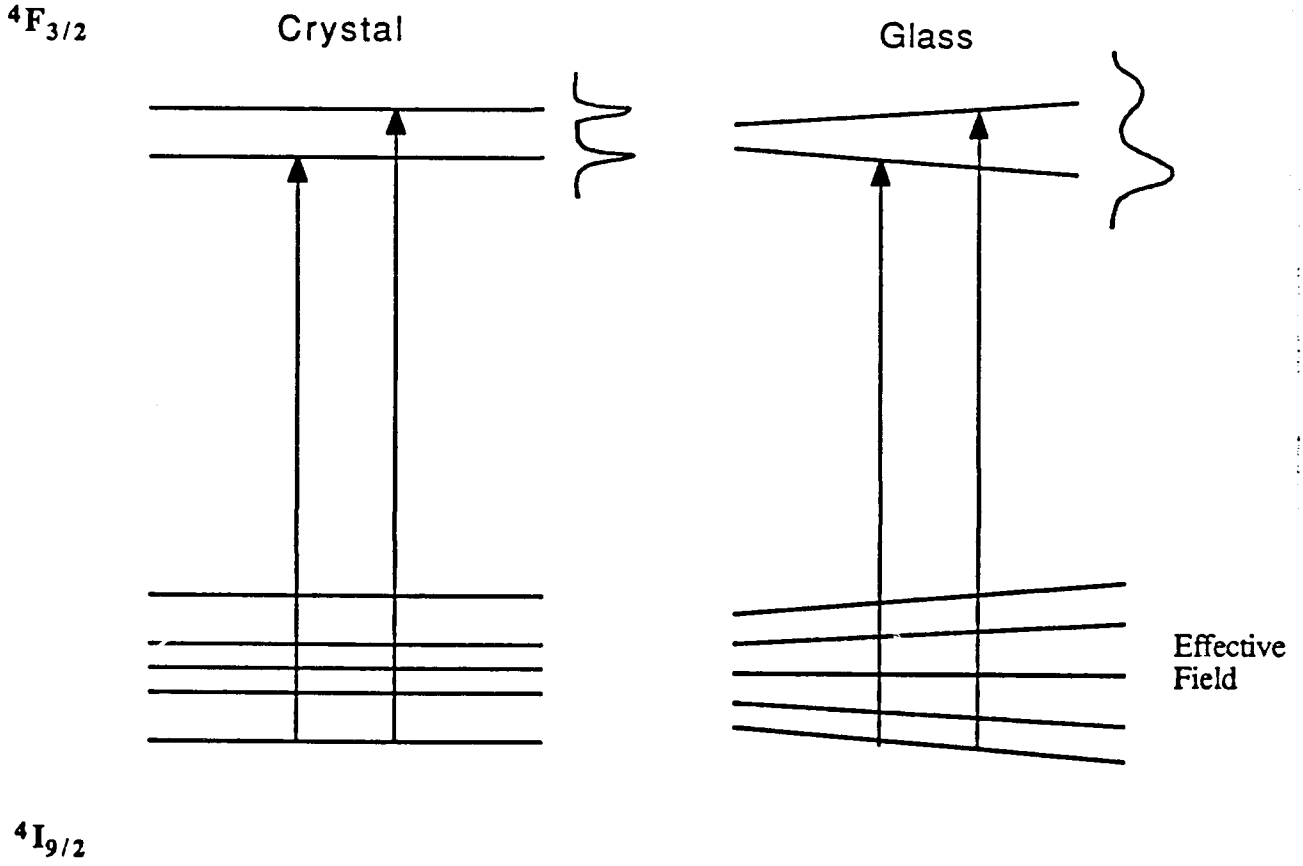

Figure 1. Schematic of $^4I_{9/2}$-$^4F_{3/2}$ Absorption Transition of Nd^{3+} in Crystal and Glass Host-Matrices and the Resulting Fluorescent Lines.

and forming the glass structure requires melting the glass at high temperatures. Platinum crucibles are normally used to minimize contamination during the melting process, but this still leads to small inclusions of platinum in the glass laser matrix that can lead to stresses in the glass and eventual laser rod destruction at high powers [5]. Crucible contamination, density fluctuations, striae, seeds, cords, bubbles and other localized inhomogeneities in the melt-glass matrix can be reduced by lowering the melting and homogenization temperature, and this is currently done by adding fluxes such as Li_2O and CaO to the SiO_2 matrix. While adding fluxes decreases the contamination and inhomogeneities associated with melting pure SiO_2, fluxes themselves can degrade the physical and optical properties of the glass, most notably the coefficient of thermal expansion and the nonlinear refractive index coefficient (see Table 1). This, along with its lower melt temperature, limits the efficiency as well as the operating temperature of the laser due to thermal gradient effects. Impurities can be a cause of solarization, which also decreases laser pump efficiency [6].

1.3 Glasses by Sol-Gel Process

Recent developments in sol-gel glass technology have permitted the fabrication of silica glasses at much lower temperatures than traditional melt glass techniques [7]. A schematic representation of the process is given in Figure 2. In this process a silicon-containing precursor, such as tetramethylorthosilicate (TMOS) or tetraethylorthosilicate (TEOS), is hydrolyzed to form a sol. After complete homogenization, this sol is cast into molds where it sets into a very porous, wet, gel having the shape of the mold. The gel is then dried to give a transparent silica monolith. The resulting dry gel can be further heat-treated to strengthen it and at the same time reduce its porosity. Although this process removes most of the water, heating to temperatures necessary to fully densify the silica gel normally results in bloating of the sample due to residual water being trapped in the porous structure. If a dehydration step is carried out before the final densification, the bloating problem is avoided and fully dense glass can be obtained [8].

TABLE 1

Properties of Commercial Silicate Glasses Used As Laser Media [1]

PROPERTY	LG-650	LG-660	LSG-91H	ED-2	COMMERCIAL SiO_2 FUSED QUARTZ	COMMERCIAL SiO_2 FUSED SILICA
Softening pt. (°C)	682	573	505	582	1630-1730	1580-1600
CTE (10^{-7})	95	121	105	92.6	5.1	5.1
Index of Refraction (589.3 nm)	1.5214	1.520	1.5612	1.5672	1.458	1.458
Non-linear Index (10^{-13}esu)	1.4	1.33	1.5	1.41	0.97	0.97
Abbe Number	56.2	58.5	56.6	58.2	67.8	67.8

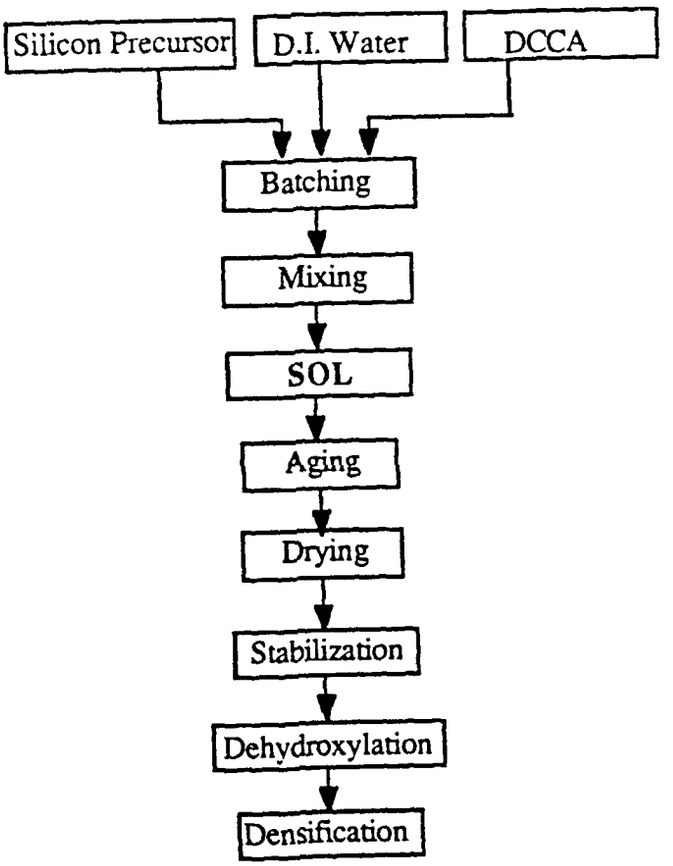

Figure 2. Flowsheet of Sol-Gel Processing of Silica Glass Monoliths.

The use of sol-gel processing to prepare solid-state laser materials holds potential advantages for the following reasons:

1. It is possible to use high purity chemical precursors that are readily available. The major cause of losses in a glass has been reported to be the presence of contaminants which absorb radiation [3].

2. Processing temperatures required to produce the glasses are substantially less than for melt glass techniques, further reducing the problem of impurities and making the process more cost effective from the standpoint of required equipment.

3. Since the process is in large part carried out on the molecular scale, it provides the potential for greater homogeneity of dopants in the glass matrix.

4. A variety of shapes are possible with the sol-gel process, since the shape is determined by the mold into which the sol is cast. This makes it possible to cast rods, discs for Brewster segments, or other geometries such as slabs, which have been used in a number of applications including amplifiers [9] and remote sensing [10]. Although shrinkage occurs in the process, it has been shown to be reproducible to within 0.5 % for each step in the process, which is important for the processing of the materials [11].

2 EXPERIMENTS

The sol-gel process lends itself to the incorporation of laser-active elements like Nd into silica glass matrix by two different methods:

1. Mixing
2. Impregnation

Procedures for fabricating Nd/SiO_2 laser glass, both by mixing and by impregnation, are detailed in Figures 3 and 4 respectively. The general process essentially involves preparing the sol, aging the sol to form a gel, drying the gel, stabilizing the gel to a porous solid, and conducting a treatment of dehydroxylation of the porous monolith before the final densification. During fabrication by mixing, the laser-active elements are added at the beginning during sol preparation, unlike the impregnation method wherein a separate solution of active elements is impregnated into a porous monolith.

2.1 Nd/SiO_2 Laser Glass by Mixing

The procedure followed for this fabrication method is shown as a flowsheet in Figure 3. Each of these steps are described in detail in the following sections.

2.1.1 Sol Preparation

The composition of the glass was selected such that it yielded 3.0 weight % of Nd_2O_3 in the glass. This composition was kept constant throughout this experiment.

The raw material precursors used for Nd/SiO_2 laser glass selected were tetramethylorthosilicate (TMOS) and tetraethylorthosilicate (TEOS) for silica (SiO_2) and $Nd(OAc)_3.H_2O$, $NdCl_3.6H_2O$ and $Nd(NO_3)_3.6H_2O$ for neodymia (Nd_2O_3). A proprietary drying control chemical additive (DCCA) was also used.

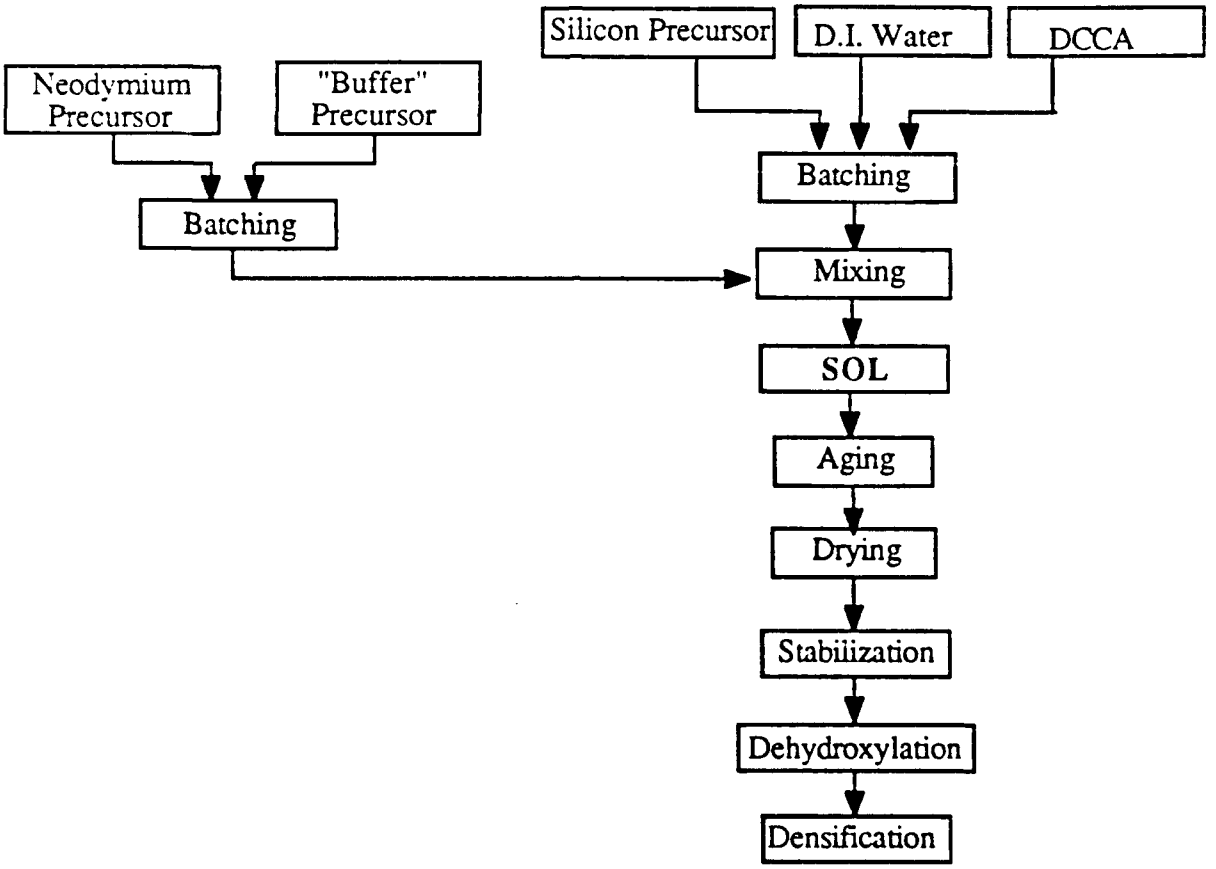

Figure 3. Flowsheet for the Sol-Gel Fabrication of Nd/SiO_2 Laser Glass by Mixing.

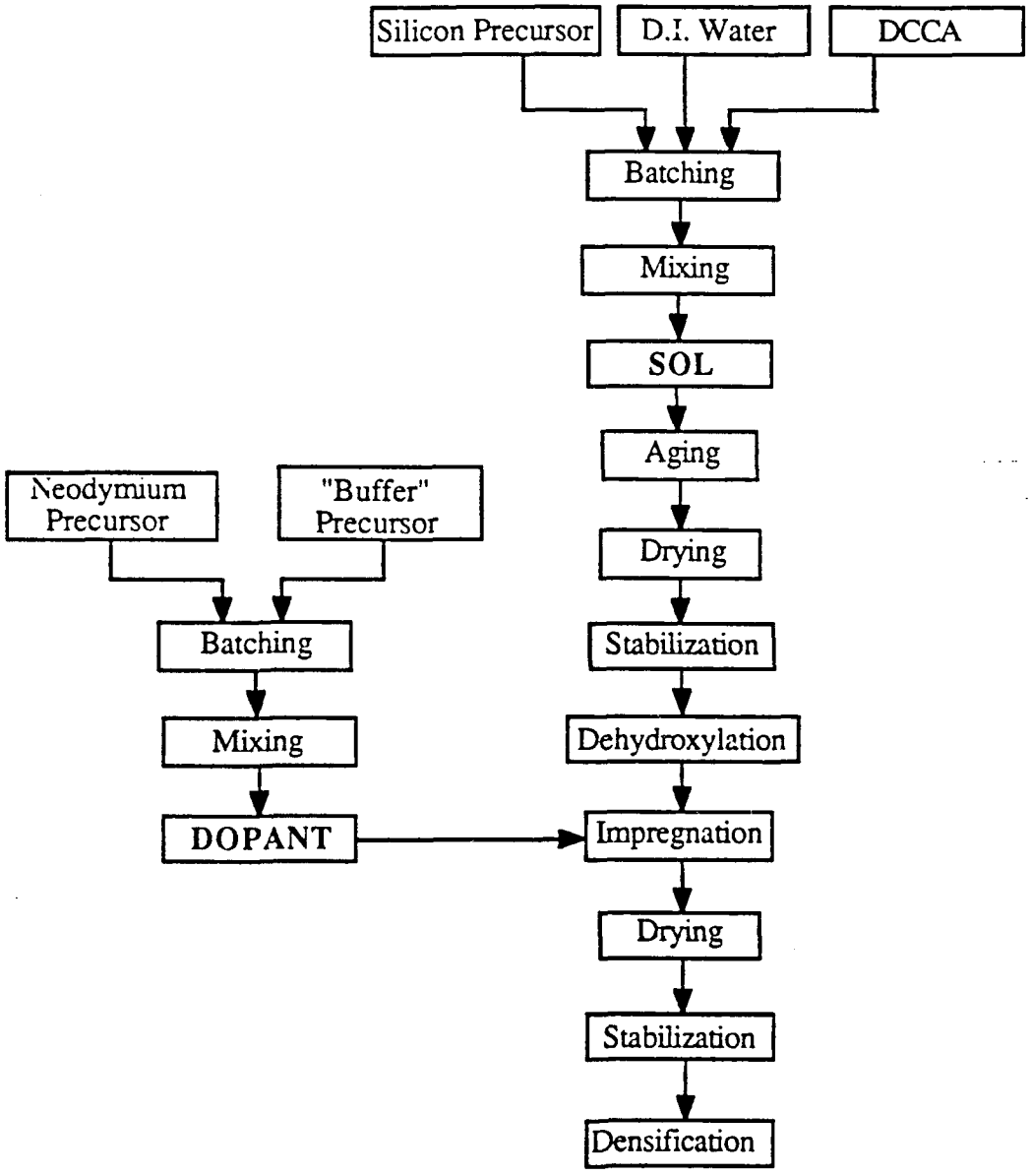

Figure 4. Flowsheet for the Sol-Gel Fabrication of Nd/SiO_2 Laser Glass by Impregnation.

The use of Al, P and Ti was explored as a "buffer" component which prevents concentration quenching of the fluorescence lifetimes of the laser-active glass.

The raw materials used were: $AlCl_3$ and $Al(OBu)_3$ for Al_2O_3; $P(OCH_3)_3$ and $PO(OCH_3)_3$ for P_2O_5; and $Ti(OPr)_4$ for TiO_2. The R ratios used were 2, 4, and 16. For the catalysis of the reactions, HCl, HNO_3 and NH_4OH were utilized.

The sols were prepared by batching them according to the requirements and mixing them in glass kettles or polypropylene beakers. Appendices IA and IB summarize the different reaction conditions present during various methods of sol preparation.

An alternative approach to making glass by using SiO_2 powder as an additive to fabricate composites was also attempted. Commercially available fumed silica was incorporated into the sol to facilitate densification of the gels. Several parameters were investigated, including particle size of fumed silica, volume percent loading of powder in the sol, use of surfactants, modifying water content of the sol, and adjusting the amount of solvent in the sol.

2.1.2 Aging & Drying

The sols obtained from above were used for the fabrication of monoliths. After casting the sol in polypropylene containers, the lids of the containers were sealed. These containers were left undisturbed for 2 days at temperatures of between 25°C and 80°C while the sol gelled into a viscoelastic solid. After gelation these wet gel monoliths were extracted from the containers and dried to yield crack-free transparent monoliths of the desired shape. These were then used for further processing.

2.1.3 Stabilization

The crack-free monoliths derived from the dried gel were further processed to remove the organic fractions from the gel. The stabilization of these monoliths was carried out

at various temperatures, all below 1200°C, to prepare monoliths with varying specific pore volume. The details of the temperatures used and the results are summarized in Appendix II. The atmosphere used was air.

2.1.4 Dehydroxylation

Various methods were used to remove the surface hydroxyl groups in the stabilized gel. First, chlorination was attempted by using CCl_4 and HCl as the chlorinating agents. Appendix III summarizes the details of the experiments. Second, a vacuum as low as 0.025 mm Hg was used. Finally, proprietary non-chlorine-containing chemicals were used for the dehydroxylation of the stabilized monoliths prior to densification.

2.1.5 Densification

The densification of the monoliths was carried out in a controlled-atmosphere furnace. The densification temperatures were kept at or in excess of 900°C and soak times were kept at one hour or greater. A variation on this experiment was the use of vacuum densification. The details of the experiments are summarized in Appendix IV.

2.2 Nd/SiO_2 Laser Glass by Impregnation

The procedure followed for this fabrication method is shown in Figure 4 as a process flowsheet. Each of the listed steps are described in the following sections in detail.

2.2.1 Sol Preparation (SiO_2 only)

The sol was prepared by mixing TMOS or TEOS, deionized water, and a proprietary drying control chemical additive (DCCA). After complete homogenization, this sol was then cast into polypropylene containers.

A variation in this experiment was to include another additive in the batch for obtaining

large pore size monoliths. The diffusion of the impregnate was expected to be facilitated by larger pore size. Several parameters and additives were investigated to find a way to get monoliths with larger pores. Variables studied were: type of catalyst, concentration of catalyst, drying method, drying schedule, silica precursor, and water content in the sol.

The approach of using silica powder in the sol, as discussed for sol preparation while making Nd/SiO_2 laser glass by mixing (section 2.1.1), was also used for fabrication of porous host-matrix.

2.2.2 Aging & Drying

After casting, the containers were left undisturbed so as to allow the sol to gel. The gelation and aging process was carried out at temperatures of between 25°C and 80°C over a 48-hour period. Following the aging process, the wet gels were dried to give a transparent ultraporous monolith.

2.2.3 Stabilization

The stabilization process involved the removal of the organic fractions from the dried monolith. This was carried out at various temperatures, not exceeding 1050°C, to prepare monoliths with specific pore sizes but with a varying specific pore volume.

2.2.4 Dehydroxylation

To remove the hydroxyl groups from the surface of the stabilized SiO_2 monolith a number of techniques were tried earlier for the samples produced by mixing. It was clear that the impregnation process will lead to the same problems which occurred with chlorination during preparation by mixing. A vacuum process with vacuum as low as 0.025 mm Hg has been investigated for the dehydroxylationof the gels. The non-chlorine-containing chemicals treatment, mentioned previously, was also used for the

dehydroxylation of the stabilized monoliths prior to densification.

2.2.5 Batching and Mixing (Nd- and Al-Precursors only)

On the basis of the pore radius, a calculation was made for the strength of the alcoholic solution which would contain enough Nd to yield 3.0 % by weight Nd_2O_3 in the SiO_2 glass. The ratio of Nd to Al was kept to a fixed number, 6. The raw materials tried for neodymium were $NdCl_3$, $Nd(NO_3)_3$, $Nd(NO_3)_3 \cdot 6H_2O$, and those for aluminum were $AlCl_3$, $AlCl_3 \cdot 6H_2O$ and $Al(NO_3)_3 \cdot 9H_2O$.

2.2.6 Impregnation

The impregnation process is essentially diffusion of the dopant liquid containing the active ions into the porous SiO_2 matrix. Impregnation is done by immersion of the porous monolith in the dopant solution. The immersion time was varied from 4 hours to 4 days.

2.2.7 Drying and Stabilization (Post-Impregnation)

The drying process following impregnation is critical. The Nd and Al ions should not migrate to the surface as that would create inhomogeneities, thereby rendering the glass unsuitable for laser applications. The drying was done at temperatures ranging from 40°C to 110°C over a period of 16 hours.

The crack-free monoliths thus produced were then stabilized at temperatures ranging from 600°C to 1000°C in a time period of 16 to 24 hours. The removal of the organics from the monoliths was carried out during this process without the cracking of gels.

2.2.8 Densification

The densification of the monoliths was carried out at temperatures greater than 1000°C.

If soaking was done at a high temperature then the soak time was in excess of 1 hour. The densification process was carried out in a controlled-atmosphere furnace.

3 RESULTS AND DISCUSSION

3.1 Optimization of the Composition

The optimization of the composition (Task 4) had the following objectives:

1. Optimization of the molar ratio of dopants.
2. Optimization of neodymium concentration.
3. Optimization of glass properties.

It is known that the molar ratio of Al_2O_3 (or P_2O_5) to Nd_2O_3 influences fluorescence properties of Nd/SiO_2 glass [12,13]. Arai et al [12] found this molar ratio to be 10 for Al_2O_3 (and 15 for P_2O_5). It was noted that this ratio was obtained for the materials prepared by chemical vapor deposition (CVD), a process very different from the sol-gel process. The percentage of neodymia (Nd_2O_3) in the glass, i.e., the Nd ion concentration, is an important parameter. This concentration must be such that the total volume of the material is excited, rather than portions thereof. The median penetration depth of the pump light should be on the order of the rod diameter to function as desired [1]. Hence, the concentration of the laser-active ions should be high enough to meet the above conditions depending on the final geometry (diameter/thickness) of the lasing element. The larger the diameter of the rod, the lower the Nd-ion concentration and vice versa. Thus, with smaller geometry lasing elements the higher limits of the concentration of Nd were being explored in this study [1].

The problem of concentration quenching, i.e., the decrease of the fluorescence lifetime with increased concentration of Nd in the matrix, was an inherent part of this study. In silicate glasses the effect of concentration quenching occurs at a lower Nd concentration than that for phosphate glasses ($\geq 2 \times 10^{20}$ ions/cc) [1].

The final thermal properties of the glass will be close to that of pure SiO_2 if the composition is not altered significantly, as shown below [12]:

Glass Composition	CTE(ppm/°C)
$0.0029Nd_2O_3 \cdot 0.029Al_2O_3 \cdot SiO_2$	0.7
SiO_2	0.5

For this study, glasses with Nd_2O_3 concentration were 5.0 weight % or less. The workhorse composition was 3.0 weight % Nd_2O_3. The corresponding concentration of active ions in the glass was ~2.0 x 10^{20} Nd ions/cc glass (~1.5 x 10^{20} Nd ions/cc for 2.0 weight % Nd_2O_3). This concentration will decrease when using the gels stabilized at a higher temperature as the specific pore volume is less for such a disk. Also, due to the composition of the glass, its CTE is expected to be closer to 0.7 x 10^{-6}/°C. A fluorescence lifetime of about 300 μs was expected, as per Figure 5 [1], for this glass.

The monoliths produced were in the form of crack-free disks of about 12 mm in diameter and about 4 mm thick. The fluorescence lifetimes of these disks were indeed close to 300 μs.

3.2 Research on Mixing Parameters

Sol-gel processing results in intimate mixing of the component materials. The level of mixing is on the molecular scale, which results in an ultra-homogeneous glass not possible via the conventional melting process. To achieve the optimized conditions for best Nd/SiO_2 laser glass, the composition of the batch and precursor is selected for a given composition.

The objectives of this study (Task 1) were as follows:

1. Maximize gel dopant retention during processing.
2. Optimize gel quality, i.e., monolithicity, clarity, and dopant homogeneity.
3. Maximize ease of densification.

4. Maximize fluorescence lifetimes.
5. Optimize thermal properties such as CTE.

3.2.1 Silica Precursor

TMOS reacted much more rapidly than TEOS, which resulted in much faster gelation times. A few experiments were conducted to compare TEOS-derived gels with those derived from TMOS. TMOS gels tended to be visibly more uniform (much less cloudy) and stronger (more resistant to cracking during drying.) TMOS was found to be much more desirable for the development of materials for optical applications.

3.2.2 Alumina Precursor

As anhydrous aluminum chloride salt was not easy to work with, therefore little time was spent pursuing this. One of the most often used compounds is aluminum sec-butoxide because it is very reactive and is a liquid at room temperature. By combining this reagent with a solution containing only partially hydrolyzed TMOS, it was possible to enhance the possibility of incorporating the aluminum into the silica network. This approach was adopted for the majority of the work on this project to date.

3.2.3 Phosphorus Oxide Precursor

The literature reports the use of phosphoric acid [14], trimethylphosphite [15,16], and triethyl-phosphate [17] in preparing glasses by sol-gel methods. However, the use of phosphoric acid caused the precipitation of neodymium phosphate when the neodymium salt was added. Trimethylphosphite did not cause precipitation at first, but as the gel formed, neodymium phosphate was excluded as a precipitate unless the amount of water was limited to two moles of water per mole of silicon precursor. However, under these conditions it was impossible to prepare monolithic gels. The best results were obtained using trimethylphosphate. The trimethyl analog was chosen over the triethyl analog for

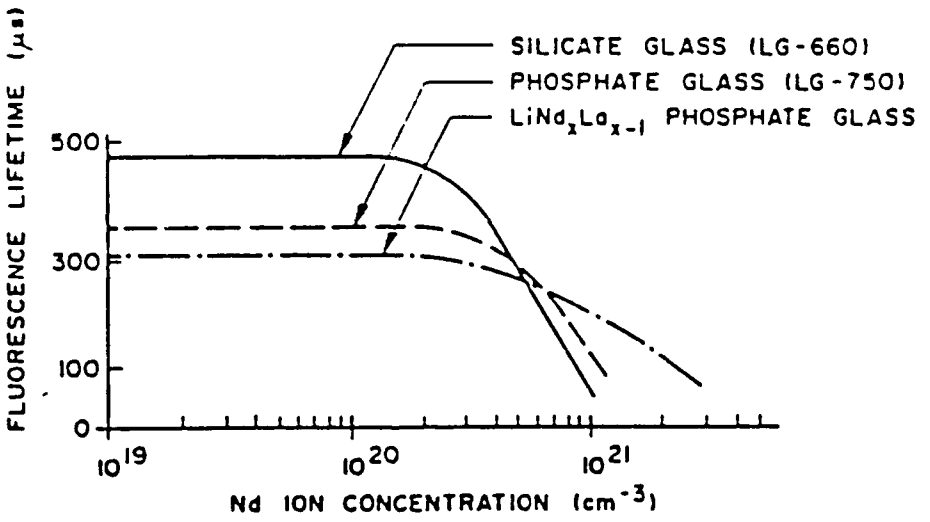

Figure 5. Effect of Nd Ion Concentration on the Fluorescence Lifetime of Various Glasses [1].

its greater reactivity. With this precursor no precipitates formed, and hence, monolithic gels were prepared containing neodymium and phosphorus oxides.

3.2.4 Neodymia Precursor

The precursor used for neodymium did not seem to make much difference in the compositions using aluminum, but when neodymium acetate was added to the batch containing phosphorus a precipitate resulted. For this reason the acetate was normally used with aluminum since it minimized the presence of inorganic ions such as nitrate or chloride when the nitrate salt was used, phosphorus was also added to avoid the precipitation problem.

3.2.5 R Ratio

The R ratio is defined as the molar ratio of water to silicon precursor. Limiting the R ratio to four gave the gels some interesting properties, particularly the tendency to densify at relatively low temperatures (700°C). This is advantageous from the standpoint of preventing crystallization in the glass.

3.2.6 Catalyst

Acid catalysts give by far the stronger gels, which is important for success in drying the gels without cracking. A prehydrolysis step using acid, followed by final condensation using either acid or base was investigated. The prehydrolysis procedure was adopted in most cases in order to enhance the opportunity to incorporate the aluminum or phosphorus into the network. When base was used after prehydrolysis the gelation times were much shorter.

3.2.7 Nd/SiO_2 Glass by Mixing

The fabrication of Nd/SiO_2 glass, containing also a "buffer" component, by mixing did

lead to crack-free disks about 8 mm in diameter and 4 mm in thickness. The disks were homogeneously doped and of good optical quality. The temperature for densification was less than 1200°C. The coefficient of thermal expansion of these monoliths is expected to remain close to that of SiO_2 glass due to their composition being so close to silica. The fluorescence lifetimes of the samples made were, however, less than 10 μs.

3.2.8 Nd/SiO_2 Glass by Impregnation

The fabrication of Nd/SiO_2 glass, with a "buffer" component, by impregnation did also lead to crack-free disks about 12 mm in diameter and 4 mm in thickness. The disks were homogeneously doped but the optical quality, in terms of scatter, was not good for lasing application. The densification was carried out at temperatures below 1300°C. The coefficient of thermal expansion is expected to be close to that of SiO_2 glass. The fluorescence lifetimes of the samples made were, however, about 300 μs. Also, these samples were made reproducibly.

3.3 Optimization of Doping

The optimization of the doping is essentially a subset of the optimization of the composition. The specific objectives of this study (Task 2) were as follows:

1. To determine which doping method gives the best fluorescence properties.
2. To determine which doping method gives the best homogeneity of the dopants.

This was a process optimization study wherein the effects of the method of sample preparation were related to the final properties of glass.

3.3.1 Nd/SiO_2 Glass by Mixing

The samples in which Nd was incorporated in silica by mixing the precursors before the

heat treatment had high uniformity and homogeneity as was evident by the color of the samples. The processing aspects of this technique are similar to that of monoliths. However, the fluorescence lifetimes of the samples thus produced were extremely low, less than 10 μs. Hence, these samples cannot be used as the media for a Q-switched laser.

3.3.2 Nd/SiO_2 Glass by Impregnation

The samples produced by impregnation were optically homogeneous when observed with the unaided eye. However, the degree of scatter observed by passing a beam of He-Ne laser through the sample disk diametrically, was relatively high. The fluorescence lifetimes were excellent in that unprecedented values of about 300 μs were measured on a series of individually prepared samples. Hence, the process was reproducible and yielded reliably high fluorescence lifetime crack-free disk samples.

3.4 *Optimization of Drying Procedures*

Drying is a critical step in the fabrication of monoliths by the sol-gel technique. It is in this step where the microcracks start to form. On further processing, these cracks propagate and cause failure of the monolith. For this study, the drying procedure contained the following objectives:

1. Optimize the fabrication of crack-free monolithic disks (and rods).
2. Optimize the procedure for clarity and homogeneity of dopants.
3. Optimize the procedure for maximum fluorescence lifetimes in gels after stabilization.

3.4.1 Nd/SiO_2 Glass by Mixing

The drying step was carried out only once in this process after the aging step (see Figure 3). During this step the "wet" gel (viscoelastic) is transformed into an

ultraporous transparent monolithic solid. The color of these monoliths was yellow to brown, depending on the dopant concentration. After stabilization to 800°C, the average radius of the pores in these monoliths was about 14 Å, the specific surface area (B.E.T.) was close to 600 m^2/g and the specific (total) pore volume was 0.4 cm^3/g.

3.4.2 Nd/SiO_2 Glass by Impregnation

In this process the drying was critical. The first drying step was done after aging the "wet" gel. The procedure used was similar to the one used in the mixing method. The resulting ultraporous monoliths, after stabilization at 800°C for example, had the same specifications as above, namely, an average pore radius of close to 14 Å, specific surface area (B.E.T.) of 600 m^2/g and specific pore volume of 0.4 cm^3/g. These stabilized monoliths were used as the host matrices for impregnation by the laser-active ions containing dopant solutions.

The following step in the process is the dehydroxylation treatment. The removal of the hydroxyl group (-OH) is essential as it interferes with, and thus weakens, the fluorescence effect of the Nd-containing lasing glass materials [1], as shown in Figure 6. This dehydroxylation is accomplished by using a non-chlorine containing compound. Crack-free ultraporous monoliths resulting after the above treatment have an extremely low concentration of hydroxyls as evidenced by UV/VIS/NIR spectral analysis (see Figure 7). A comparison of this spectrum with that of densified SiO_2 prepared by sol-gel, as shown in Figure 8, indicates a presence of residual hydroxyls, ~135 parts per million in concentration.

The final drying step was carried out after the impregnation with the dopant solution. In this step, the cracking tendency of the host matrix (ultraporous monolith) was highest due to the stresses generated in the pores, which are severe. The deposition of the Nd- and Al-salts on the (internal) surfaces of pores and the stresses due to the drying front of the dopant solution are extremely high. Despite these problems, crack-free monolith disks were fabricated by modifying the drying program used for these drying steps.

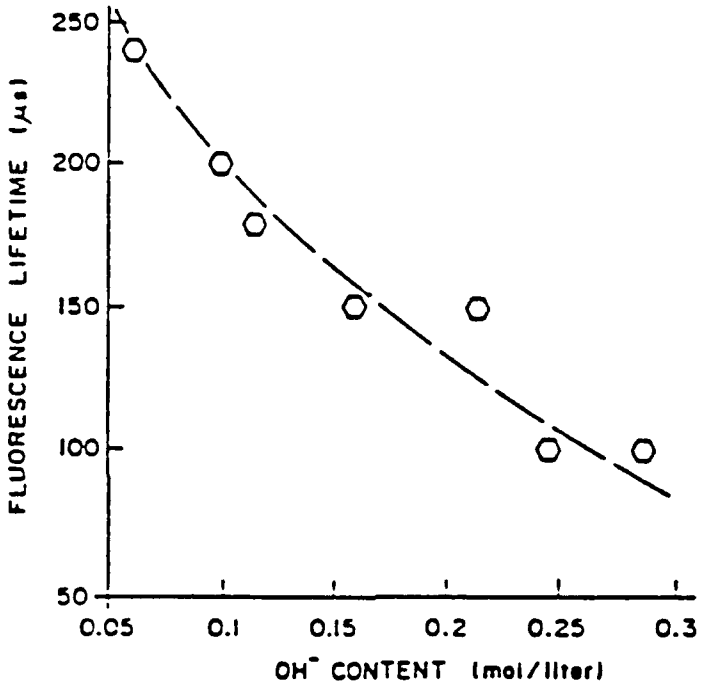

Figure 6. Dependence of Fluorescence Lifetime on Hydroxyl Content of a Nd-Phosphate Glass.

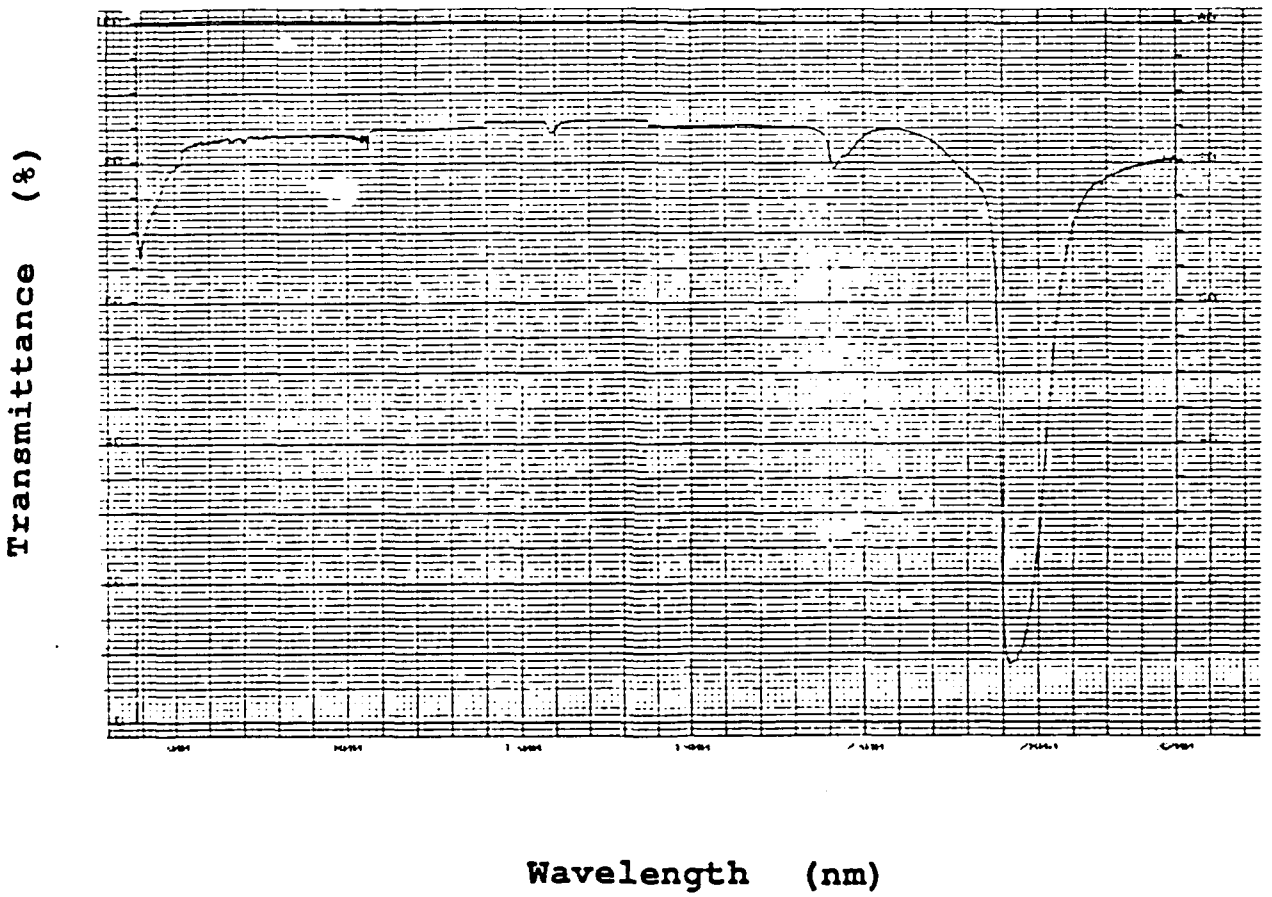

Figure 7. Transmittance Spectrum of Ultraporous "Dehydroxylated" Silica Host-Matrix.

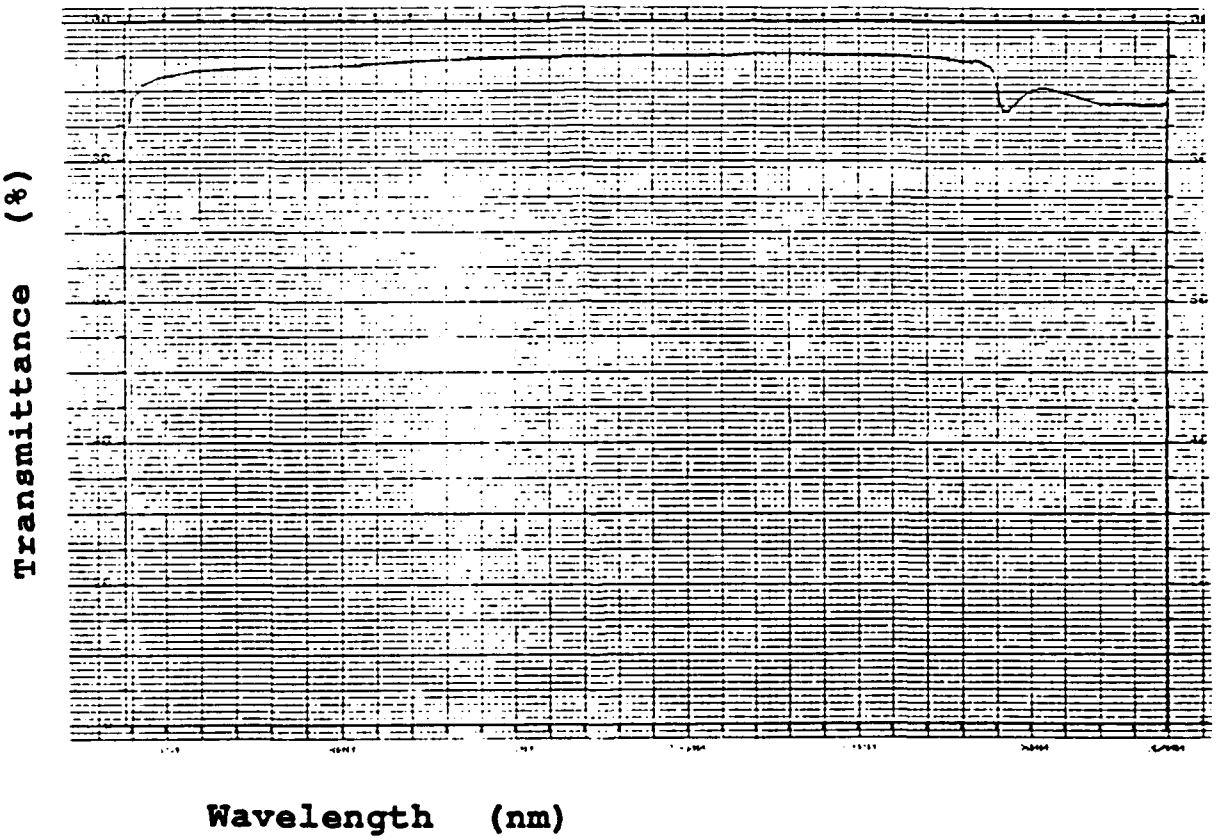

Figure 8. Transmittance Spectrum of Densified Silica Glass.

However, these drying programs could not be used for the rods (which have a much higher aspect ratio compared to the disks) without developing cracks. Thus, the geometry of the monolith has a strong influence on the drying characteristics of the monoliths. The specific bulk surface area seems to have a drastic effect during this processing step and warrants further study.

3.5 Optimization of Dehydroxylation & Densification

As mentioned earlier, the presence of hydroxyls (-OH groups) can weaken the fluorescence effect. Hence, minimization of the concentration of these hydroxyls is warranted. The objectives of this optimization procedure (Task 5) were as follows:

1. Determine if the presence of water has a deleterious effect on the fluorescence lifetimes of the gels.
2. Optimize schedules and conditions to give minimum water content in the gel after complete densification.
3. Optimize schedules to prevent crystallization in the gel.
4. Optimize optical quality of the dense gel.

The effect of water in laser material is a parameter which is not totally clear in the literature. In some cases -OH can cause a shortening of the fluorescence lifetimes, but these results were for an entirely different matrix [18]. It has also been reported that in the preparation of silicate laser glasses the absorbed water of raw materials when less than 0.2 weight % has no effect [19]. The effect of water in the glass on fluorescence lifetimes was investigated. Water content could be measured on thin slices, or if necessary, on a portion of the material which has been crushed and examined in another matrix such as KBr. The 2730 nm transmission in the near infrared has been used to quantify the presence of -OH in silica glasses [20].

3.5.1 Dehydroxylation with Chlorine

Processing of silica glass via sol-gel methods normally requires a dehydration treatment prior to pore closure [8]. Some form of chlorine is most often used [21]. Chlorine can be generated in the furnace using carbon tetrachloride. This approach was thoroughly investigated for the multicomponent gels under consideration by varying the treatment conditions. Even the lowest temperature used gave unsatisfactory results. If the chlorine reacted with the sample it caused degradation of the gels to a powdery white, opaque material. Both chlorine gas and hydrogen chloride gas were investigated as alternative dehydrating agents, but with similar, undesirable results. Gels containing aluminum, phosphorus, or titanium as a third component all reacted similarly.

X-ray diffraction of the white material did not indicate crystallization present, so electron diffraction was performed using the transmission electron microscope, but still no crystallization was detected.

3.5.2 Dehydroxylation by Vacuum

There has been very little published regarding the use of a vacuum in sintering sol-gel glasses. As a first level of investigation, a primary vacuum system was set up using a tube furnace. The best vacuum achieved was approximately 25 μm Hg. Different heating schedules were tested, including both a very slow schedule and a very fast one (200°C/h). In neither case was the procedure adequate to completely remove the water. The best results were obtained using the fast schedule. However, the results were very similar when the experiments were repeated using only static air. At this point, the expense of a hard vacuum system prohibited further investigation of this technique.

3.5.3 Dehydroxylation by Non-Chlorine Chemicals

Due to the inability of the chlorine-based dehydroxylation processes to remove the hydroxyl groups from the silica matrix irreversibly, new systems for dehydroxylation

were explored. A treatment with non-chlorine chemicals was used for this purpose. Figure 7 shows the UV/VIS/NIR spectrum of the matrix after the treatment with this chemical. As noted from this figure 7, the range of amount of hydroxyl groups is only about 135 parts per millions. Such ultraporous samples were used as the host-matrices for Nd/SiO_2 glass samples prepared by impregnation. Even though the temperatures were close to 1200°C, there was some degree of porosity left in the monoliths. Even though less than 5.0 %, this porosity can seriously deteriorate the performance of the laser media in adverse environment.

3.5.4 Densification of Sol-Derived Monoliths

The densification of sol-gel materials is very dependent on initial processing. For example, Al_2O_3/SiO_2 gels prepared with aluminum isopropoxide and TEOS resulted in 50 Å pore radii after drying, and densified without foaming to produce a clear, monolithic glass [22]. Previous work indicated that gels doped with only neodymium could be heated to densities greater than those of pure silica without foaming. In this study, the behavior of the gels prepared by various methods of mixing and doping was investigated during densification to determine the best route to full densification.

Figure 9 shows the results of DTA of 5.0 weight % Nd_2O_3 dried gel powder. An endotherm was observed between 50°C and 150°C due to loss of absorbed water. Between 250°C and 400°C, an exotherm was observed due to the oxidation of the organic fractions from the gel. At a temperature close to 1100°C an exotherm, which corresponds to crystallization, was observed [23]. The detailed characteristics of Nd-doped gels after heat treatment are listed in Appendix III.

The specific surface area and total pore volume decrease with increasing temperature of heat treatment, as shown in Figure 10, especially beyond 800°C. Also, Figure 11 shows that the sample bulk density and the shrinkage increase with increasing temperature with the effect being more pronounced beyond 800°C. Clearly, the behavior of these multicomponent gels is very similar to that of pure silica [11].

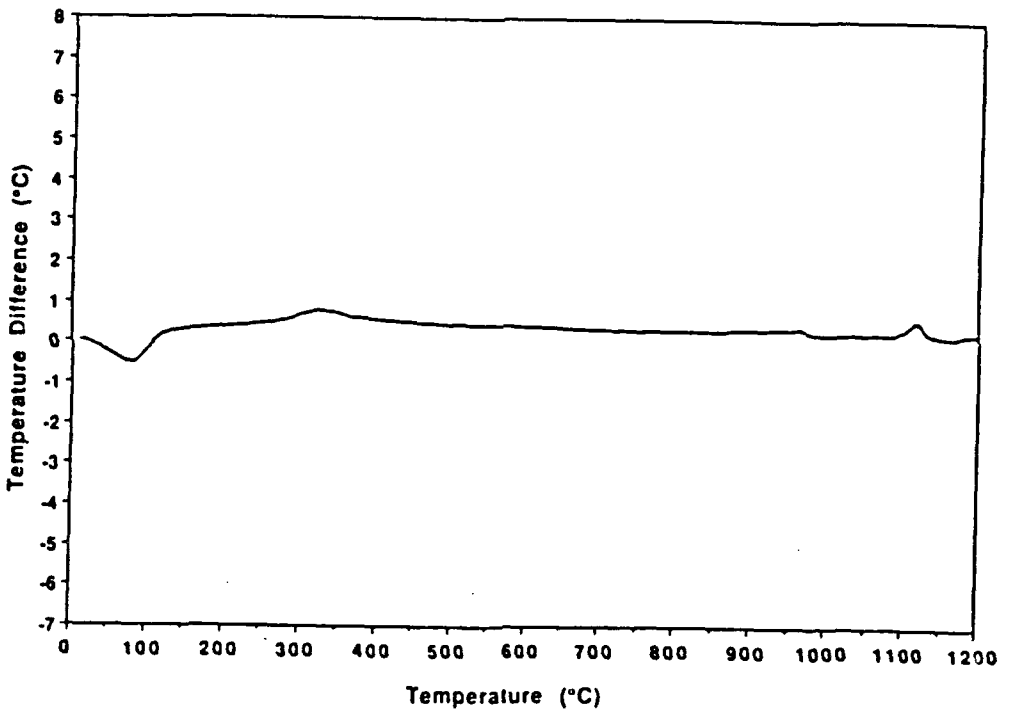

Figure 9. Differential Thermal Analysis of Nd/Al/SiO_2 Dried Gel Powder.

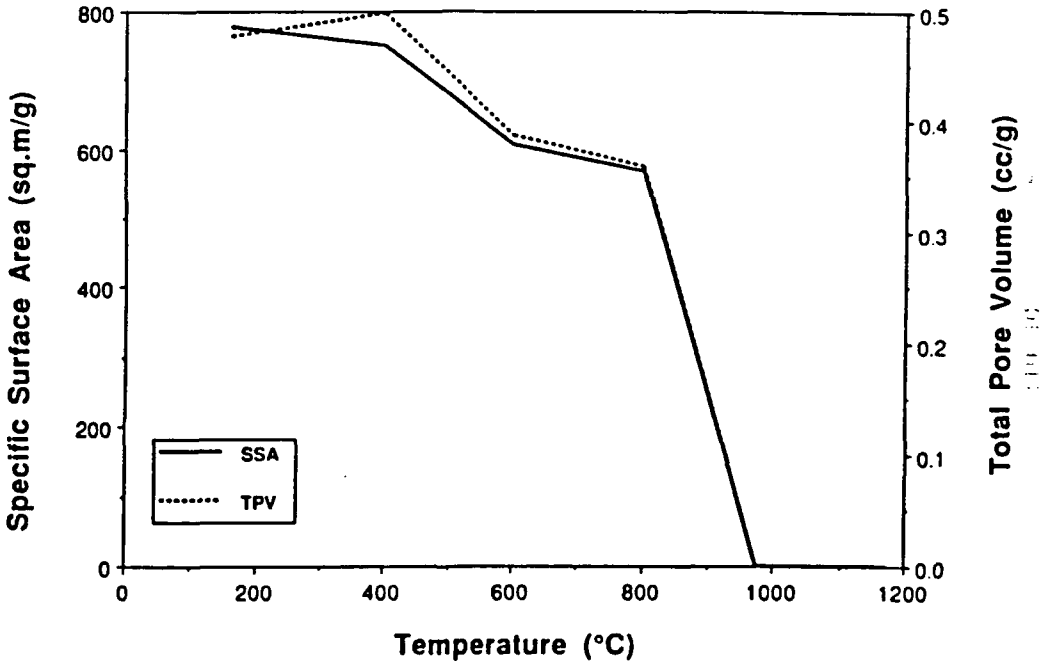

Figure 10. Specific Surface Area (SSA) and Average Sample Shrinkage (ASS) as a Function of Densification Temperature.

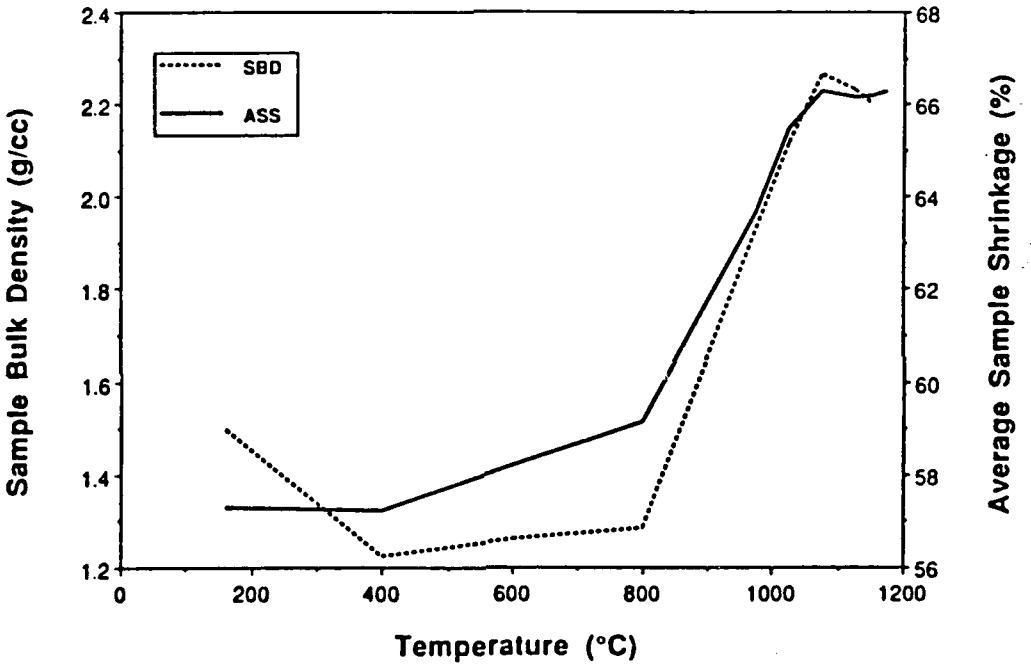

Figure 11. Sample Bulk Density (SBD) and Average Sample Shrinkage (ASS) as a Function of Densification Temperature.

TEM analysis of samples with varying amounts of Nd_2O_3 in SiO_2 glass showed clumping of the Nd ions. The average size of the clusters was around 100 nm. A representative microstructure of the Nd/SiO_2 glass is shown in Figure 12 for a 5.0 weight % Nd_2O_3 in silica glass prepared by the sol-gel technique. The fluorescence lifetimes for these samples were less than 10 μs. Such low lifetimes were attributed to the concentration quenching in these glasses.

Arai et al [12] found that addition of "buffer" elements like Al or P in the Nd/SiO_2 glass produced by CVD improves the fluorescence lifetime drastically. Using these elements, and the sol-gel method, samples with lifetimes between 90 μs and 110 μs could be fabricated. The fluorescence spectrum of such a glass is shown in Figure 13. Note that the maximum intensity is at 1.06 μm, characteristic of Nd/SiO_2 glass. Thus, the behavior of fluorescence was relatively unaffected by the addition of slight amounts of "buffer" elements [11]. These results of higher fluorescence lifetimes were, however, not reproducible.

The fluorescence lifetime of the samples formed by impregnation gave reproducible results for fluorescence lifetimes of ~300 μs. The samples were in the form of crack-free disks, 12 mm in diameter and 4 mm in thickness. Figure 14 shows the comparison of the temporal profiles of 1.06 μm fluorescence from a $Nd/Al/SiO_2$ laser glass fabricated at GELTECH by the sol-gel method and a commercial Nd-silicate laser glass made by conventional melting.

3.5.5 Densification of Silica Powder Derived Composites

Silica powder has been used successfully to prepare fully dense silica glass by dispersing the powder in the sol prior to gelation [24]. This approach makes it possible to densify the glass by allowing for removal of much more of the water prior to pore collapse. This method was applied to Nd/SiO_2 by both the mixing and the impregnation techniques.

Figure 12. Transmission Electron Micrograph of a 5.0 weight % Nd_2O_3 in Silica Glass Prepared by Sol-Gel at 20,000x.

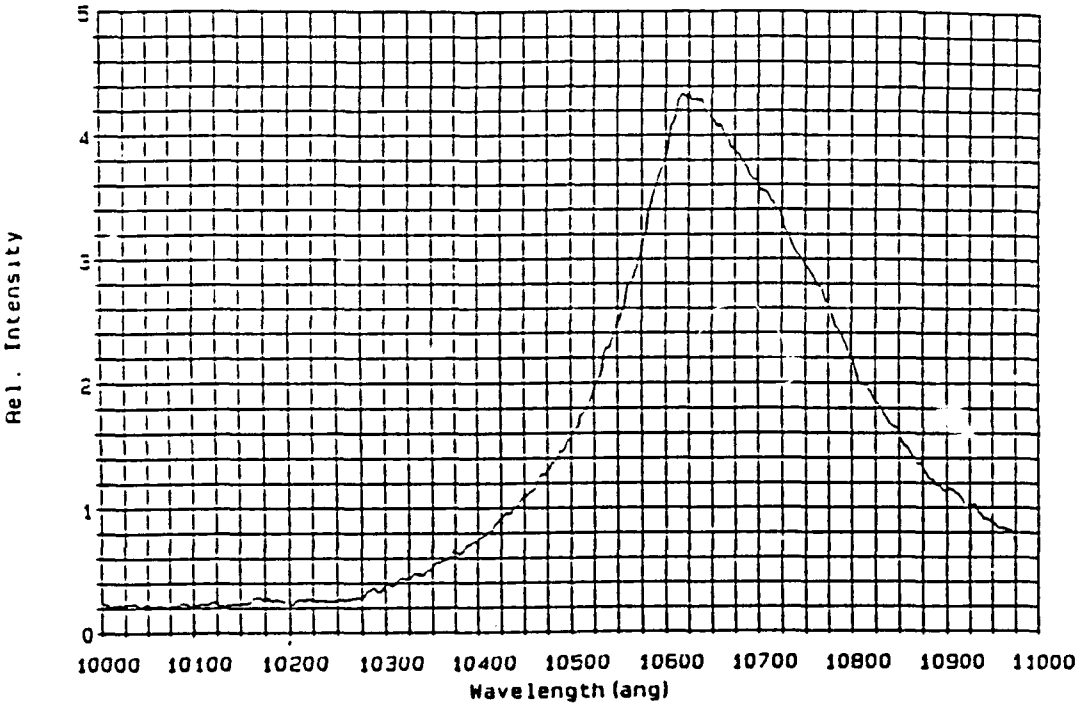

Figure 13. Fluorescence Spectrum of 3.0 weight %.Nd/Al/SiO_2 Glass.

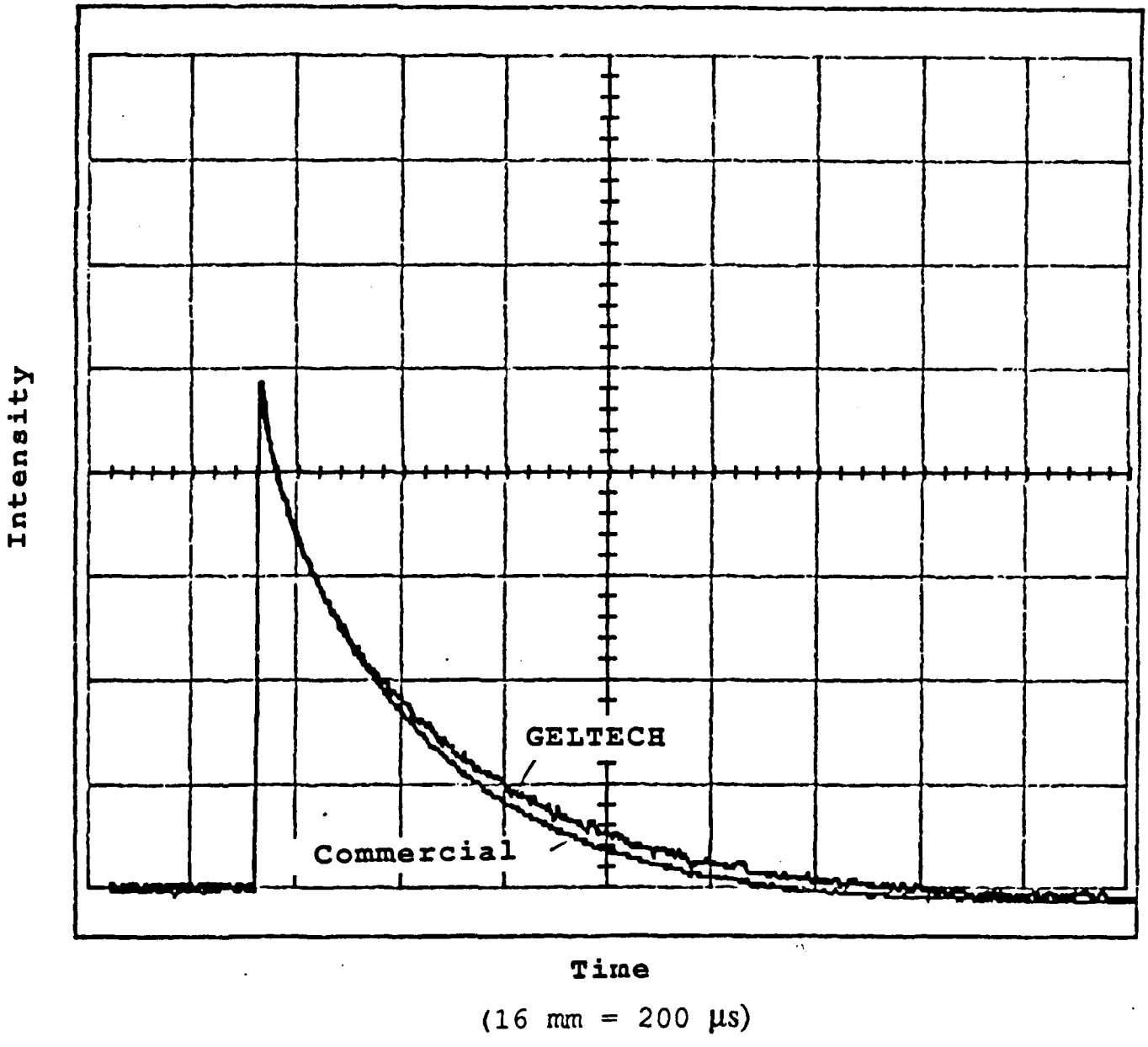

Figure 14. Temporal Profiles of the 1.06 μm Fluorescence from Nd/Al/SiO_2 Laser Glass by Sol-Gel and a Commercial Nd-silicate Laser Glass by Conventional Melting

Silica powder was mixed with the multicomponent sol prior to gelation and sonicated to aid dispersion. After gelation the gels were dried and fired to 1350°C. Unfortunately the resulting material was opaque and bluish-white. This occurred in gels containing only neodymium, as well as neodymium and aluminum. However, it could not be ascertained as to whether this was due to the crystallization. Similar problems persisted when silica composite host matrices were used for impregnation. Hence, this method was not used any further.

3.6 Addition of Sensitizers

The addition of sensitizer ions to a matrix containing laser-active ions is done so that it can absorb energy which is not absorbed by the laser-active ion and which can be later transferred for laser action. The efficiency and power output of a laser can be increased by adding small amounts of other ions which absorb the pump radiation and efficiently transfer it to the appropriate energy level of the lasing species [25]. A number of various ions have been used as sensitizers with Nd^{+3}, including Ce^{+3}, Cr^{+3}, Mn^{+2}, UO_2^{+2}, and $(VO_4)^{-3}$ [26]. However, this phenomenon appears to be influenced by the laser host material, since in one report co-doping with Ce^{+3}, UO_2^{+2}, Eu^{+2}, Tb^{+3}, and Cr^{+3} in a phosphate laser material resulted in significant gains from only the Tb^{+3} [27]. It was found that the efficiency of Cr^{+3} as a sensitizer of Nd^{+3} in phosphate glasses was very dependent on the glass composition [28]. In essence, the sensitizer boosts the energy efficiency of the laser. For example, Cr ions transfer their excitation energy to Nd ions with 45.0 % efficiency [1]. Ions of other elements like Yb and Er are important sensitizers. The objectives of this study (Task 6) are as follows:

1. Determine which sensitizer ions increase the fluorescence lifetime of neodymium in a sol-gel matrix.
2. Determine the optimum concentration of these ions for sensitization.
3. Examine the properties of the glasses containing the sensitizers to determine what effect, if any, a small concentration of the sensitizers will have on glass properties such as CTE.

3.6.1 Erbium as a Sensitizer

Erbium was successfully incorporated in the sol-gel derived dehydroxylated SiO_2 host matrix. The incorporation technique was by impregnation as used for Nd previously. A buffer element, Al, was also used as in the case of Nd. The densification temperature was kept at 1100°C. No foaming was observed either, which attests to the incorporation of the sensitizer, if done in a manner similar to the laser-active Nd ion, poses no extra problems in processing. Figures 15 and 16 show the transmittance spectra of partially densified $Nd/Al/SiO_2$ and $Er/Al/SiO_2$ glasses, respectively. Note that the absorption peaks, all of which are below 1.0 μm, show that those for the Er sensitizer incorporated via sol-gel method behaved in a manner similar to that in glass fabricated by commercial melting.

The level of concentration of the sensitizer and its effect on the thermal properties could not be optimized as the focus remained on the fabrication of crack-free, larger geometry rods.

3.7 Demonstration of Production of Doped Monoliths

The Phase II program of the fabrication of Nd/SiO_2 laser glass had as its end result the attainment of the following objectives (Task 7):

1. Scale-up the laboratory experiments to pilot plant scale.
2. Demonstrate repeatability and reproducibility on scale-up.

While we could successfully fabricate Nd/SiO_2 glass with fluorescence lifetimes of ~300 μs reproducibly and reliably, this was possible only for disk geometries which were obtained in crack-free form. Rods, which have a high aspect ratio, could not be fabricated in crack-free form in the given time period. The issue of optical quality of the final product could also not be addressed because of the time constraints. Another

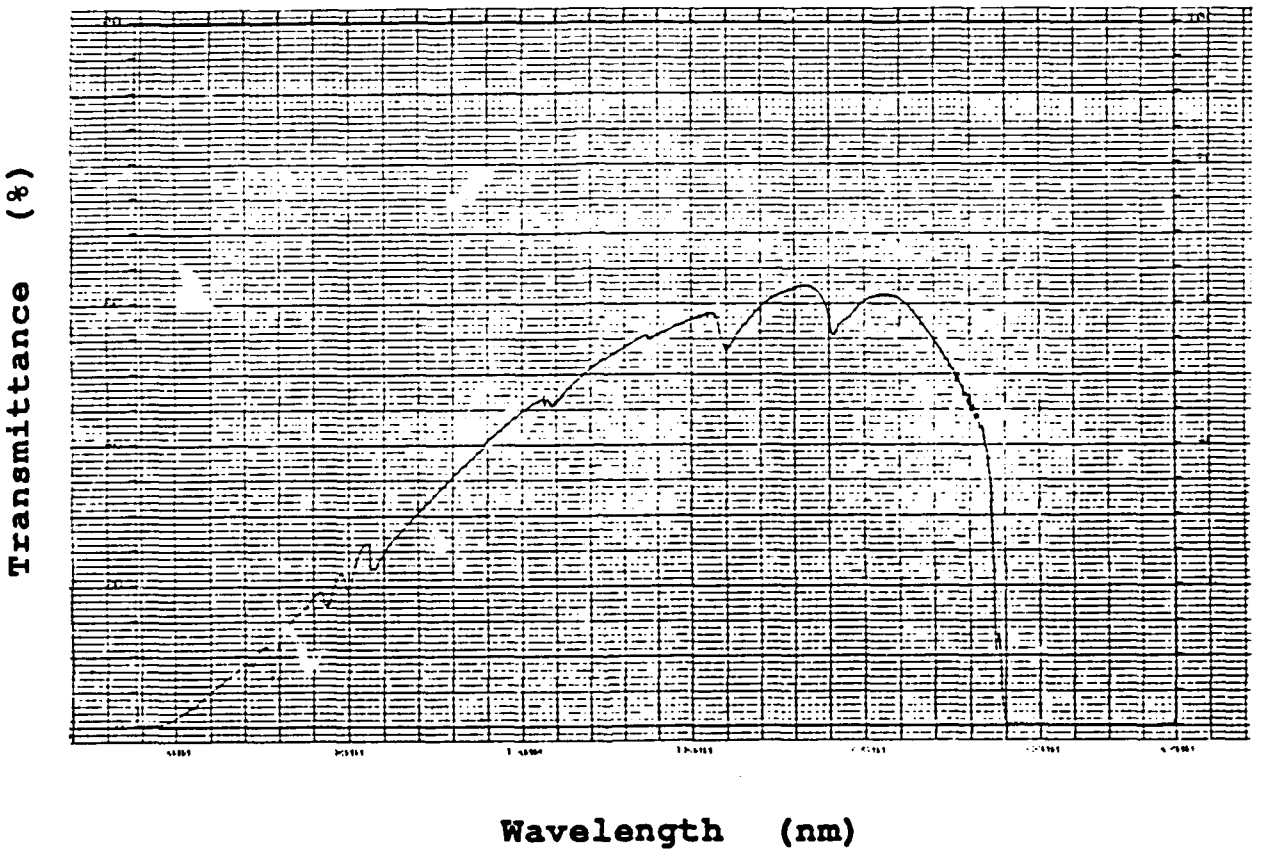

Figure 15. Transmittance Spectrum of Porous Nd/Al/SiO_2 Glass.

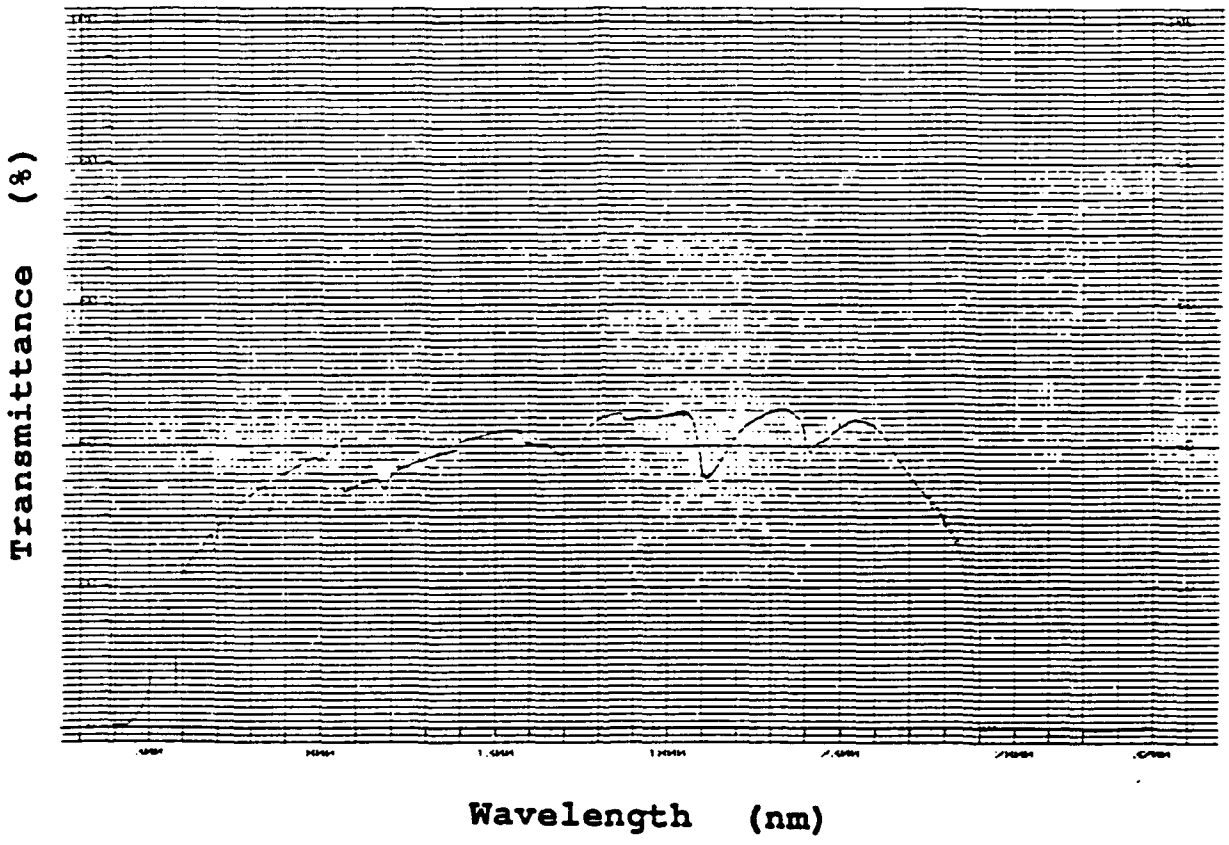

Figure 16. Transmittance Spectrum of Porous Er/Al/SiO_2 Glass.

issue, the influence of batch size on the scaled-up procedure, was also not pursued due to inadequate time.

4 CONCLUSIONS

This research effort has successfully developed a reproducible procedure for the fabrication of crack-free monolithic disks of 3.0 weight % Nd-doped silica glass with fluorescence lifetimes close to 300 μs. The size of these disks was 12 mm in diameter and 4 mm in thickness. Larger size, high aspect ratio geometry samples like rods were difficult to fabricate reproducibly in crack-free form. The successful procedure involved first, the fabrication of ultraporous silica monolith; second, its dehydroxylation to minimize the concentration of hydroxyls which interfere with 1.06 μm fluorescence of Nd/SiO_2 glass; third, impregnation of laser-active Nd^{3+} ions with a buffer element Al to prevent cluster quenching which reduces fluorescence lifetime; and, lastly, densification of the matrix to produce a solid-state lasr glass media. Erbium could also be incorporated as a sensitizer successfully by sol-gel technique. Further process development is warranted to address the issues of optimization of the sensitizer and the optical quality, in greater detail, to fabricate large size rods for high efficiency Q-switched lasers.

5 REFERENCES

1. N. Neuroth, *Optical Engineering*, 26 [2] 96-101 (1987).
2. S. E. Stokowski, "Glass Lasers", in *Handbook of Laser Science and Technology*, M.J. Weber, ed.,CRC Press, 215-264.
3. E. Snitzer, *Applied Optics*, **5** [10] 1966, 1487-1499.
4. E. Snitzer, *Am. Ceram. Soc. Bull.*, **52** [6] 516-525 (1973).
5. R. W. Hopper and D. R. Uhlmann, *J. of Applied Physics*, **41**(10) 1970 4023-4037.
6. J. M. Buzhinskii and S. K. Mamonov, *Journal of Applied Spectroscopy*, **8**, 1968, 438-442. *Zhurnal Prikladnoi Spektroskopii*, **8**(5), 1968, 731-737.
7. I. Matsuyama, K. Susa, S. Satoh, and T. Suganuma, *Bulletin of the American Ceramic Society*, **63**(11), 1984, 1408-1411.
8. J. Phalippou, T. Woignier, and J. Zarzycki, pp. 70-87 in *Ultrastructure Processing of Ceramics, Glasses, and Composites*, L. L. Hench and D. R. Ulrich, eds., John Wiley & Sons, NY, 1984.
9. A. Varanavicius, R. Grigonis, R. Danielius, A. Piskarskas, and D. Podenas, *Kvantovaya Elektron*, **13**(12), 1986 2391-2395. Chem. Abstracts **106**:146658z
10. R. L. Byer, T. Kane, J. Eggleston, and S. Long, *Springer Series in Optical Sciences*, **39**, 1983, 245-256. Chem. Abstracts **8**:R184675b.
11. W. V. Moreshead, *Development of a High Efficiency Q-Switched Glass Laser via Sol-Gel Processing*, SBIR Phase I Final Technical Report, contract #F49620-87-C-0087, submitted to AFOSR, 1988.
12. K. Arai, H. Namikawa, K. Kumata, T. Honda, Y. Ishii, and T. Handa, *J. Appl. Phys.*, **59**[10] 3430-3436 (1986).
13. B. J. Ainslie, S. P. Craig, and S. T. Davey; *Mater. Lett.*, **5** [4] 143-146 (1987).
14. I. Thomas, US Patent No. 767-432, 1973.
15. T. Woignier, *Ph. D. Dissertation*, University of Montpellier, Montpellier, France, 1984.
16. T. Woignier, J. Phalippou, and J. Zarzycki, *Journal of Non-Crystalline Solids* ,

63 117-130(1984).

17. F. Tian, L. Pan, and X. Wu, *Journal of Non-Crystalline Solids,* **104** 129-134(1988).
18. I. A. Zhmyreva, I. V. Kovaleva, V. P. Kolobkov, and B. V. Tatarintsev, *Journal of Applied Spectroscopy,* **29**, 1978, 1119-1123. *Zhurnal Prikladnoi Spektroskopii,* **29**(3), 1978,515-520.
19. I. M. Buzhinskii, S. F. Geichenko, E.I. Koryagina, and V. F. Surkova, *Opt.-Mekh. Prom-st.*, **4**,1982, 58-59. Chem. Abstracts **97**:136427e.
20. J. E. Shelby, J. Vitco Jr., and R. E. Benner, *Comm. of Amer. Cer. Soc.*, **65**(4) 1982, C-59.
21. M. P. McDaniel, J. Phys. Chem., **85**[5] 532-541(1981).
22. D. M. Krol and J. G. van Lierop, *Journal of Non-Crystalline Solids* **63**, 1984, 131-144.
23. W.V. Moreshead, J.R. Noguès, and R.H. Krabill, *J. Non-Cryst. Solids*, **121** 267-272 (1990).
24. S. Miyashita, S. Kanbe, M. Toki, T. Takeuchi, H. Kitabayashi, Japanese Patent Application # JP 61/168540 (1985).
25. L. F. Johnson, L. G. Van Uitert, J. J. Rubin, and R. A. Thomas, *Phys. Rev.*, **133**,1964, A 494-498.
26. M. J. Weber , "Lanthanide and Actinide Lasers", pp. 275-311in *Lanthanide and Actinide Chemistry and Spectroscopy*, N. M. Edelstein, ed., Amer. Chem. Soc., DC, 1980.
27. J. D. Myers, *Energy Res. Abstr.*, **2**(20), 1977.
28. V. P. Gapontsev, A. K. Gromov, A. A. Isineev, V. B. Kravcenko, S. M. Matytsin, M. R. Sirtlanov, and N. S. Platonov, *Proc. Int. Conf. Lasers*, 1982 (Pub. 1983), 310-314. Chem. Abstracts **102**:53554q.

Appendix IA

Aluminum as the "Buffer" Component

Representative Batch Name	SiO_2 Precursor	Al Precursor	Nd Precursor	R Ratio	Catalyst	Fluorescence Lifetime(μsec)
NA88-4101	TMOS	$AlCl_3$	$NdCl_3$ -$6H_20$	16	HCl	
NA88-4301	TMOS	$AlCl_3$	$NdAc_3$ -H_20	16	HCl	
NA88-4901	TMOS	$Al(OBu)_3$	$NdAc_3$ -H_20	16	HNO_3	
NA88-5101	TMOS	$Al(OBu)_3$	$NdAc_3$ -H_20	16	HNO_3	<10
NA88-5301	TMOS	$Al(OBu)_3$	$NdAc_3$ -H_20	16	HNO_3	<10
NA88-5303	TMOS	$Al(OBu)_3$	$NdAc_3$ -H_20	16	HNO_3	<10
NA89-0301	TMOS	$Al(OBu)_3$	$NdAc_3$ -H_20	4	HNO_3/NH_3	
NA89-0501	TMOS	$Al(OBu)_3$	$NdAc_3$ -H_20	16	HNO_3/NH_3	<10
NA89-0505	TMOS	$Al(OBu)_3$	$NdAc_3$ -H_20	4	HNO_3	<10
NA89-0602	TMOS	$Al(OBu)_3$	$NdAc_3$ -H_20	4	NH_3	<10
NA89-1601	TEOS	$Al(OBu)_3$	$NdAc_3$ -H_20	16	HNO_3	
NA89-1602	TEOS	$Al(OBu)_3$	$NdAc_3$ -H_20	16	HNO_3/NH_3	
NA89-3401	TMOS	$Al(OBu)_3$	$NdAc_3$ -H_20	16	HNO_3	
NA89-3501	TEOS	$Al(OBu)_3$	$NdAc_3$ -H_20	16	HNO_3	

Appendix IB

Phosphorus as the "Buffer" Component

Representative Batch Name	SiO_2 Precursor	P Precursor	Nd Precursor	R Ratio	Catalyst	Fluorescence Lifetime(μsec)
NP88-5001	TMOS	$(OCH_3)3P$	$NdAC_3$ -H_2O	16	HNO_3	
NP88-5202	TMOS	$(OCH_3)3P$	$Nd(NO_3)$-$6H_2O$	2	HNO_3	
NP89-0301	TMOS	$(OCH_3)3P$	$Nd(NO_3)$-$6H_2O$	2	HNO_3/NH_3	
NP89-0401	TMOS	$(OCH_3)3PO$	$Nd(NO_3)$-$6H_2O$	16	HNO_3	<10
NP89-0601	TMOS	$(OCH_3)3PO$	$Nd(NO_3)$-$6H_2O$	4	HNO_3/NH_3	<10
NP89-1101	TMOS	$(OCH_3)3PO$	$Nd(NO_3)$-$6H_2O$	16	HNO_3	<10
NP89-1103	TMOS	$(OCH_3)3PO$	$Nd(NO_3)$-$6H_2O$	16	NH_3	
NP89-1203	TMOS	$(OCH_3)3PO$	$Nd(NO_3)$-$6H_2O$	16	HNO_3/NH_3	<10
NP89-1602	TMOS	$(OCH_3)3PO$	$Nd(NO_3)$-$6H_2O$	4	HNO_3/NH_3	

Titanium as the "Buffer" Component

Representative Batch Name	SiO_2 Precursor	Ti Precursor	Nd Precursor	R Ratio	Catalyst	Fluorescence Lifetime(μsec)
NT88-5101	TMOS	$Ti(OPr)_4$	$Nd(OAc)_3 \cdot H_2O$	16	HNO_3	<10

GELTECH, Inc. • One Progress Blvd., Box 18, Alachua, FL 32615 • USA TEL: (904) 462-2358 • FAX: (904) 462-2993

APPENDIX II

Characteristics of Nd-doped Gels versus Densification Temperature

Temperature (°C)	SSA (m^3/g)	TPV (cm^3/g)	SBD (g/cm^3)	ASS (%)
160	777	0.477	1.50	57.28
400	751	0.499	1.22	57.22
600	607	0.388	1.26	58.20
800	569	0.359	1.28	59.15
975	BDL	BDL		63.68
1025	BDL	BDL	2.12	65.47
1075	BDL	BDL	2.27	66.28
1125	BDL	BDL	2.23	66.13
1150	BDL	BDL	2.20	66.17
1175	BDL	BDL		66.28

Legend:

SSA: specific surface area
TPV: total pore volume
SBD: sample bulk density
ASS: average sample shrinkage
BDL: below detection limit

GELTECH, Inc. • One Progress Blvd., Box 18, Alachua, FL 32615 • USA TEL: (904) 462-2358 • FAX: (904) 462-2993

APPENDIX III

Dehydroxylation by Chlorine-Based Chemicals

Run #	Chemical Composition	Chlorine Source	Temp. (°C)	Time (h)	Results
TF 23.2	Nd/SiO_2 $Nd/Ti/SiO_2$	CCl_4	310	68.30	Cracked, starting to turn opaque White, greenish, opaque
TF 26.2	$Nd/Al/SiO_2$	CCl_4	310	66.50	Spectrum after treatment: Shows no improvement
TF 27.2	$Nd/Al/SiO_2$	CCl_4	463	50.75	Spectrum after treatment: Shows no improvement
TF 49.2	$Nd/P/SiO_2$	CCl_4	700	18.00	Spectrum after treatment: Shows no improvement
TF 51.2	$Nd/P/SiO_2$	CCl_4	500	25.50	Broken, thin slice from surface dehydrated some, bulk saturated
TF 53.2	$Nd/P/SiO_2$	CCl_4	470	62.75	Cracked, ran spectrum after treatment: Thin slice still had OH.
TF 56.2	$Nd/P/SiO_2$	CCl_4	600	15.50	Gels powdery, bluish, opaque
UF 01	Nd/SiO_2 $Nd/Al/SiO_2$	Cl_2	875	3.00	Cracked, starting to turn opaque Broken, bluish white, opaque
TF 30.2	$Nd/Al/SiO_2$	HCl	650	25.00	Broken, starting to turn opaque
TF 43.2	$Nd/Al/SiO_2$ $Nd/P/SiO_2$	HCl	700	9.00	Bluish white, opaque Cracked, starting to turn white
TF 39.2	$Nd/Al/SiO_2$ $Nd/P/SiO_2$	HCl	850	30.00	Bluish white, opaque, some breakage Foamed, broken.

APPENDIX IV

Vacuum Sintering of Sol-Gel Silica (Doped)

Run #	Max. Temp. (°C)	Rate (°C/h)	Vacuum (μm Hg)	Chemical Composition	Results
VF 1.2	1000	75	750	Nd/P/SiO_2	Foaming
VF 2.2	1100	5	≤4	Nd/Al/SiO_2 Nd/P/SiO_2	Foaming
VF 3.2	950	5	≤20	Nd/Al/SiO_2 Nd/P/SiO_2	Foaming
VF 4.2	900	5	≤20	Nd/Al/SiO_2 Nd/P/SiO_2	Saturated with Water
VF 6.2	1050	200	≤100	Nd/P/SiO_2	Saturated with Water
VF 7.2	1050	200	None	Nd/P/SiO_2	Saturated with Water
VF 8.2	1100	200	None	SiO_2 (Larger Pores)	Foaming

APPENDIX A

Journal of Non-Crystalline Solids 121 (1990) 267–272
North-Holland

PREPARATION, PROCESSING, AND FLUORESCENCE CHARACTERISTICS OF NEODYMIUM-DOPED SILICA GLASS PREPARED BY THE SOL–GEL PROCESS

William V. MORESHEAD, Jean-Luc R. NOGUÈS and Robert H. KRABILL [1]

Geltech, Inc., One Progress Blvd. #18, Alachua, FL 32615, USA

For high-powered laser applications silica glass has favorable thermal and mechanical properties. However, the limited solubility of neodymium oxide in silica has prevented its use without the addition of other components, both to increase the solubility of the neodymium oxide and to reduce processing temperatures, minimizing impurities such as platinum inclusions. The preparation of up to 20 wt% Nd-doped silica has been reported recently using the sol–gel process, and the fluorescence spectrum of a one weight per cent composition was given (E.J.A. Pope and J.D. Mackenzie, J. Non-Cryst. Solids 106 (1988) 236). In this paper, the preparation and thermal processing of 3–5 wt% compositions, including BET, density, thermal and spectral analyses, are reported. The fluorescence spectrum of the material and its fluorescence lifetime are then correlated with TEM/EDS results.

1. Introduction

Silica glass has many favorable properties for use in high-powered glass lasers, such as: (1) a broad transmission range from ultraviolet to infrared; (2) a low nonlinear index of refraction; and (3) a low coefficient of thermal expansion. However, the high processing temperatures required and the low solubility of neodymium oxide in silica have prevented the preparation of such glasses with reasonable amounts of neodymium oxide without the addition of other elements to the glass. The addition of these other elements greatly diminishes the desirable properties of the glass for use as a laser host. In 1973 Stone and Burrus [2] reported the preparation of silica fibers doped with 0.5 wt% Nd_2O_3, but only recently, Pope and Mackenzie have reported the preparation of Nd-doped silica containing up to 20 wt% Nd_2O_3 using the sol–gel process [1]. The sol–gel process holds some potential advantages for this application because of: (i) processing temperatures lower than those used in traditional melt glass techniques; (ii) better control of purity; and (iii) the potential for greater homogeneity on a molecular scale since it involves the mixing of precursors at low temperatures ($< 100\,^{\circ}C$).

The preparation, structural evolution, and visible and fluorescence spectra of 3–5 wt% glass prepared by the sol–gel process are reported. In addition the fluorescence lifetimes are given and correlated with TEM results.

2. Experimental

Tetramethylorthosilicate (TMOS, Petrarch, Inc.) was mixed with deionized water in which was dissolved neodymium nitrate (Aldrich, Inc.). After complete homogenization, this sol was cast into 60 mm petri dishes where it was allowed to gel and age between room temperature and $80\,^{\circ}C$ over a period of about two days. The wet gel was then dried to give a transparent gel monolith. Further heat treatment was carried out to study the evolution in properties with temperature. Samples were removed at desired temperatures and quenched in air.

Differential thermal analysis was performed on a Dupont Instruments 910 DTA connected to a 1090 Thermal Analyzer. The sample was heated at a rate of $10\,^{\circ}C$/min up to a temperature of

[1] Present address: American Matrix, Inc., 118 Sherlake Drive, Knoxville, TN 37922 USA.

1200 °C, and alumina was used as the reference. After each temperature treatment, the textural characteristics of the sol–gel monoliths were measured using an Autosorb-6 from Quantachrome Corporation, and the results were analyzed according to the BET theory.

The density measurements were performed on oven-dried samples using a normal specific gravity bottle, with mercury being used as the liquid for displacement. Values given represent the average of at least seven repetitions. The shrinkage of the samples was determined by measuring the diameter of the disc-shaped monoliths after each of the selected temperatures. A minimum of two measurements of the diameter was done per sample using a digital caliper with an accuracy of ± 0.01 mm. The visible absorption spectra of the sol–gel samples were recorded on a Lambda-9 spectrophotometer from Perkin–Elmer. Fluorescence spectra and fluorescence lifetimes were measured. Transmission electron microscopy was also performed.

3. Results and discussion

3.1. Visual characteristics

All the sol–gel samples were transparent, reddish purple, and monolithic after processing except those heated to 1150 and 1175 °C, which became white and opaque with the onset of foaming.

3.2. Differential thermal analysis

Figure 1 shows the results of the differential thermal analysis of a 5 wt% composition. At least three features can be seen: (1) an endotherm between 50 and 150 °C due to loss of absorbed water; (2) an exotherm between approximately 250 and 400 °C, due to the burning of organic residues; and (3) an exotherm between 1050 and 1100 °C, which gives evidence of crystallization.

3.3. Textural and physical characteristics

The textural and physical characteristics of the samples are summarized in table 1. These gels show trends with heat treatment very similar to pure silica [3]. As the gels are heated the specific surface area and total pore volume decrease while the bulk density and the shrinkage of the samples increase. Changes in each of these characteristics follow a similar trend, changing slowly until the temperature reaches 800 to 850 °C, and then changing much more quickly as pore closure occurs. Finally, if the heating is continued, foaming due to the release of OH trapped in the pores after closure begins. Figures 2 and 3 show these trends. One noticeable distinction between the Nd-doped gels and the pure silica is the ability to heat the

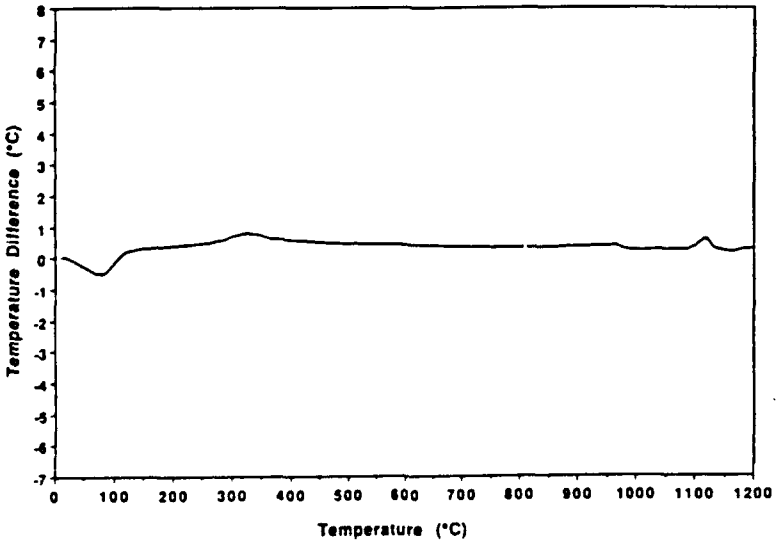

Fig. 1. Differential thermal analysis of a Nd : gel.

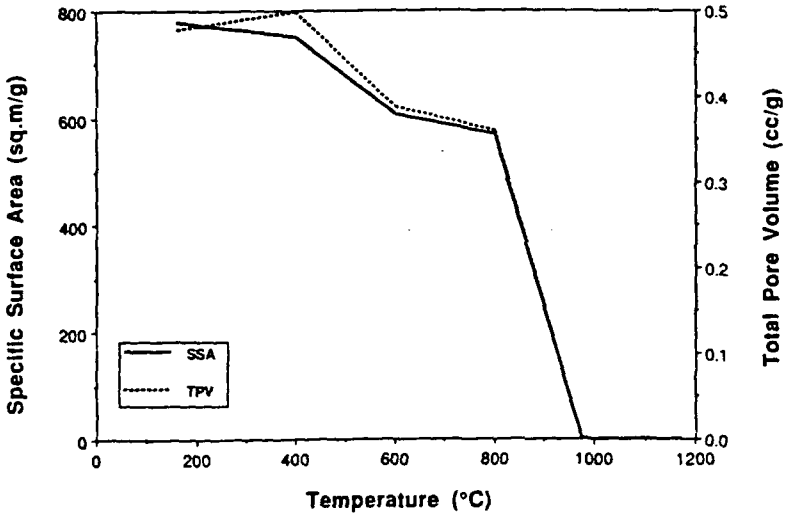

Fig. 2. Specific surface area (SSA) and total pore volume (TPV) versus densification temperature.

doped samples to higher temperatures before foaming occurs. Also, during the thermal treatments the doped gels appeared to be less susceptible to cracking and/or crazing.

3.4. Visible spectroscopy

Absorption of the gels was measured after several treatment temperatures to observe the evolution of the environment of the neodymium in the matrix. Pope and Mackenzie indicated that for a 5% composition the peak position representing the $^4I_{9/2}$ to $^4F_{5/2}$ transition shifted from 794 to 806 nm as treatment temperature increased, reaching a maximum at a temperature of 200 °C [1]. For the 5% gels described in this paper this behavior was not observed. Instead, the shift occurred over the entire range of temperatures until the maximum of 1150 °C was reached, although the shift was less significant above ~ 500 °C. This result is understandable, however, considering the fact that several changes are taking place over this temperature range. Not only are the burning of organic residues and dehydration of the gel occur-

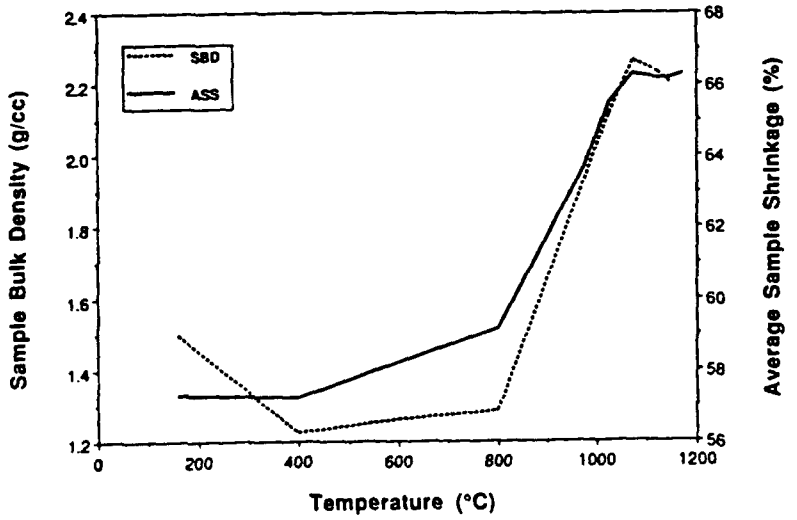

Fig. 3. Sample bulk density (SBD) and average sample shrinkage (ASS) versus densification temperature.

Table 1
Characteristics of Nd-doped gels versus densification temperature

Temperature (°C)	SSA (m^3/g)	TPV (cm^3/g)	SBD (g/cm^3)	ASS (%)
160	777	0.477	1.50	57.28
400	751	0.499	1.22	57.22
600	607	0.388	1.26	58.20
800	569	0.359	1.28	59.15
975	BDL	BDL		63.68
1025	BDL	BDL	2.12	65.47
1075	BDL	BDL	2.27	66.28
1125	BDL	BDL	2.23	66.13
1150	BDL	BDL	2.20	66.17
1175	BDL	BDL		66.28

SSA: specific surface area; TPV: total pore volume; SBD: sample bulk density; ASS: average sample shrinkage; BDL: below detection limit.

ring, but the neodymium nitrate is decomposing and the neodymium oxide is forming clusters or aggregates due to solubility limits, as is discussed below. Neodymium nitrate reportedly decomposes first to the oxynitrate, but not until it reaches 830 °C is it completely converted to the oxide [4].

3.5. *Fluorescence spectroscopy and lifetimes*

A representative fluorescence spectrum of a neodymium-doped gel having 3 or 5 wt% neodymia is presented in fig. 4. This spectrum shows a maximum emission near 1.06 μm, which is typical for neodymium oxide in silicate glasses (see fig. 4). For concentrations near 1 wt% neodymium oxide in silica, the maximum is reported to occur at 1.08 μm [2,5].

Measurement of the fluorescence lifetimes gave very low values: on the order of 5 to 7 μs, as opposed to values greater than 150 μs for commercial laser glasses. A lifetime greater than 100 μs is necessary to make the glass commercially usable. These low values are presumably due in part to concentration quenching of the neodymium, as described by Namikawa et al. [6]. Because neodymium oxide is immiscible in silica glass in the composition range from around 2–26 wt% [7], it forms aggregates or clusters in which cross relaxation can give rise to non-radiative de-excitation of neodymium, resulting in very short lifetimes. Clustering of the neodymium in the glass would also explain why the maximum emission in the fluorescence spectrum is similar to that of a silicate glass. The neodymium oxide-rich regions are apparently behaving more as a silicate glass than a doped silica matrix. These results are in agreement with those of Arai et al., who prepared neodymia–silica glasses by plasma torch CVD [8]. Another factor contributing to the short lifetimes is no doubt a high concentration of water in the gel, which has also been shown to shorten the fluorescence decay [9].

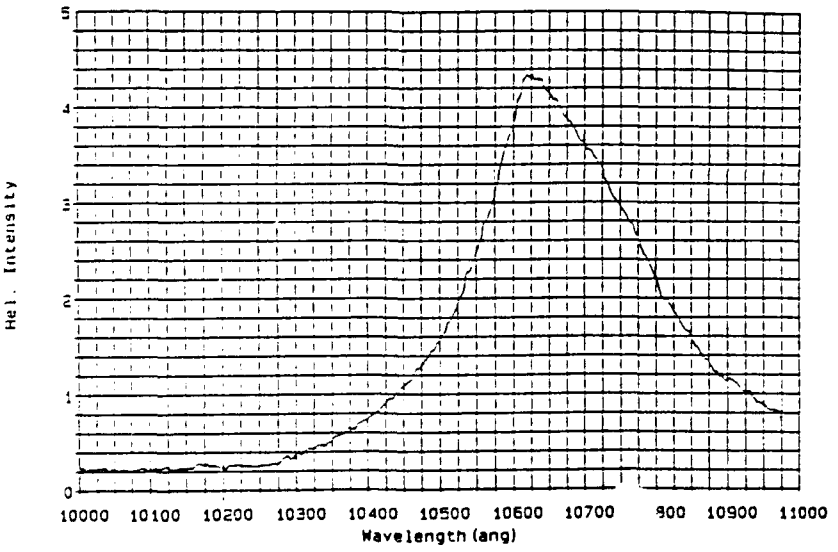

Fig. 4. Fluorescence spectrum of 3 wt% neodymium oxide–silica glass.

3.6. Transmission electron microscopy

In order to demonstrate further the existence of neodymium oxide aggregation in the silica matrix, TEM was carried out on a sample. It was found that these clusters could be seen by observing the thin edge of a powdered sample. Figure 5 shows a TEM micrograph of a neodymium-doped sample. More extensive characterization of these neodymium-doped samples has been carried out at the University of Manchester, UK using both TEM and EDS [10]. Using EDS to measure the Nd concentration in both the clusters and the matrix, the clusters were found to be rich in neodymium, and show some evidence of crystallinity. The concentration of Nd_2O_3 in the matrix was much lower.

Preliminary investigations to solve the immiscibility problem are underway at Geltech, Inc., in collaboration with the University of Manchester team. Galant et al. [11] have demonstrated laser action in quartz glass after the addition of a small amount of a 'buffer component', which does not greatly diminish the desirable thermal properties of the silica host. Arai et al. [12] have shown using the CVD process that aluminium or phosphorus can be used as this third component to disperse more homogeneously the neodymium oxide and eliminate the concentration quenching. Initial results at Geltech, Inc. have shown that the addition of a few per cent of either of these codopants reduce to a large extent the formation of clusters. Prototype samples with lifetimes between 90 and 110 μs have been produced, showing a possibility for the development of a laser material.

Fig. 5. Transmission electron micrograph of a 5 wt% neodymium oxide–silica glass.

4. Conclusion

The use of the sol–gel process to make neodymium-doped laser glasses for high power applications was investigated. Samples of 3–5 wt% neodymium oxide were prepared and their structural evolution was followed over a range of temperatures using differential thermal analysis, BET, shrinkage, density, and visible spectroscopy. The fluorescence spectrum and fluorescence lifetimes were given and the results further explained using transmission electron microscopy. The fluorescence spectrum was shown to be typical of a silicate glass matrix, with lifetimes far too short to be useful for laser action. These short lifetimes were attributed to concentration quenching of the neodymium and quenching by the high concentration of water in the matrix. Although the sol–gel process allows the preparation of much higher concentrations than the melt process, the usefulness of these materials for laser applications is limited by the immiscibility of neodymium oxide in silica glass. Research is currently underway to develop potential laser materials having a small per cent of a third component to solve the immiscibility problem and lengthen fluorescence lifetimes without greatly changing the desirable properties of silica as a host glass.

The encouragement of Dr D.R. Ulrich is gratefully acknowledged along with the financial contribution of contracts from SDI and AFOSR. The research was sponsored by Air Force Office of Scientific Research (AFSC), under contract #F49620-89-C-0006. The United States Government is authorized to reproduce and distribute reprints for governmental purposes notwithstanding any copyright notation hereon. The authors also wish to thank Drs John Daly and Bill Williams of Litton laser Systems, Apopka, FL for measuring the fluorescence spectra and lifetimes, and E.J. Jenkins of Microanalytical Laboratories, Gainesville, FL for carrying out the transmission electron microscopy.

References

[1] E.J.A. Pope and J.D. Mackenzie, J. Non-Cryst. Solids 106 (1988) 236.
[2] J. Stone and C.A. Burrus, Appl. Phys. Lett. 23 (1973) 388.
[3] J.L. Noguès and W.V. Moreshead, these Proceedings, p. 136.
[4] W. Wendlandt, Anal. Chim. Ac. 15 (1956) 435.
[5] B.J. Ainslie, S.P. Craig and S.T. Davey, Mater. Lett. 5 (1987) 143.
[6] H. Namikawa, K. Arai, K. Kumata, Y. Ishii and H. Tanaka, Jpn. J. Appl. Phys. 21 (1982) L360.
[7] M.K. Resered, Phase Diagram for Chemists 1969 Supplement (The American Ceramic Society, Columbus, 1969).
[8] K. Arai, H. Namikawa, K. Kumata, Y. Ishii, H. Tanaka and I. Iida, Jpn. J. Appl. Phys. 22 (1983) L397.
[9] I.M. Buzhinskii, S.F. Geichenko, E.I. Koryagina and V.F. Surkova, Opt.-Mekh. Promst. 4 (1982) 58.
[10] A.J. Berry and T.A. King, in Proc. US–UK Optical Glass and Macromolecular Materials Symp., Pitlochry, Scotland, 1988 (Hoechst Celanese Corporation, Somerville, NJ, 1988).
[11] E.I. Galant, Yu.N. Kondrat'ev, A.K. Przhevuskii, T.I. Prokhorova, M.N. Tolstoi and V.N. Shapovalov, JETP Lett. 18 (1973) 372.
[12] K. Arai, H. Namikawa, K. Kumata, T. Honda, Y. Ishii and T. Handa, J. Appl. Phys. 59 (1986) 3430.

APPENDIX B

V.K. Seth, W.V. Moreshead and J.L. Noguès, "Enhanced Fluorescence Lifetime of Nd/SiO_2 Glass Fabricated via Sol-Gel"

Manuscript is in preparation, and will be submitted to Materials Letters.

APPENDIX C

J. Phys. D: Appl. Phys. 22 (1989) 1419–1422. Printed in the UK

Characterisation of doped sol–gel derived silica hosts for use in tunable glass lasers

A J Berry and T A King

Physics Department, Schuster Laboratory, Manchester University, Manchester M13 9PL, UK

Received 10 April 1989

Abstract. Measurements of laser-relevant properties of neodymium doped sol–gel derived silica hosts are described. Samples with Nd as the only dopant reveal anomalously short fluorescence lifetimes characteristic of concentration quenching, TEM measurements revealing clumping of the neodymium. Co-doping with aluminium allows better dispersion of the neodymium throughout the gel–silica matrix, but fluorescence lifetimes and efficiencies are still lower than expected. Phonon quenching by residual OH^- ions is suspected, absorption, FTIR and Raman spectroscopy being used to support this theory.

1. Introduction

The ability to dope sol–gel derived silica hosts with controlled amounts of a lasing species affords the possibility of developing a new generation of advanced tunable solid state lasers. Such lasers, as well as possessing the limited tunability common to all glass lasers, can also take advantage of the superior physical properties of sol–gel derived silica. These properties include: low non-linear refractive index coefficient; low strain birefringence; coefficient of thermal expansion close to zero; low temperature dependence of expansion coefficient and low impurity levels.

As a first step towards the construction of a working laser it is necessary to investigate the laser-relevant properties of the doped sol–gel derived silica hosts of interest. These properties are indicated by the equation for the population inversion density required for lasing threshold (Yariv 1976)

$$N_2 - N_1 = N_t = \frac{8\pi n^3 \tau \Delta\nu}{c t_c \lambda^2}$$

where τ is the spontaneous lifetime of the upper lasing level. $\Delta\nu$ is the linewidth of the transition and t_c is the loss-dependent cavity lifetime. To reach threshold easily, therefore, one requires low losses, narrow linewidth and short lifetimes. For tunability, however, the linewidth needs to be large. Thus, one needs low losses and short lifetimes. It is crucially important, however, that the effective lifetime is the spontaneous lifetime and not a much shorter lifetime resulting from non-radiative quenching processes which drastically reduce the fluorescence efficiency and thereby increase the pump energies needed. Initial experiments in this study have therefore concentrated on measuring the fluorescence lifetimes, linewidths and efficiencies of variously doped gel–silica samples.

The samples themselves were manufactured by Geltech Inc., Florida, USA and generally took the form of small discs or cylindrical rods. Neodymium was the obvious lasing element to investigate first, the preponderance of Nd–glass laser systems testifying to its superior lasing qualities. The well known $^4F_{3/2} \rightarrow {}^4I_{11/2}$ transition at about 1.06 μm has the highest gain and typically has a bandwidth of $\approx$30 nm in a silicate-based glass (Levine 1968). It therefore represents the best chance of obtaining tunable operation of this new class of solid state glass lasers. Dopants of possible future interest will include other rare earths, such as erbium and holmium, and various transition metals, particularly chromium.

2. Experimental method

A standard pulsed excitation and wavelength-selective temporal observation technique was employed consisting of a flashlamp-pumped dye laser (FPDL), sample, monochromator, filter, PMT and storage oscilloscope. Neodymium has a convenient absorption at 585 nm, a wavelength easily accessed by a FPDL operating on the dye Rh6G. 200 mJ pulses could be obtained with durations of ~2 μs FWHM, much shorter than the expected fluorescence lifetimes. A PMT with an S1 photocathode was used to detect fluorescence at about 1.06 μm, as well as fluorescence at about 900 nm from the

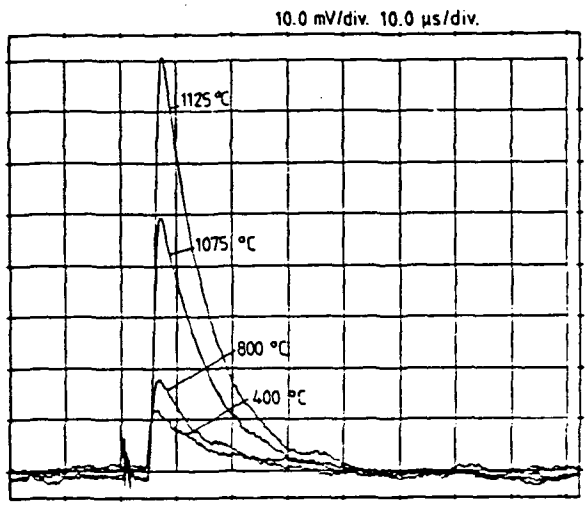

Figure 1. Temporal profiles of the 1.06 μm fluorescence from 5 wt% Nd_2O_3 doped gel–silica samples densified to different temperatures.

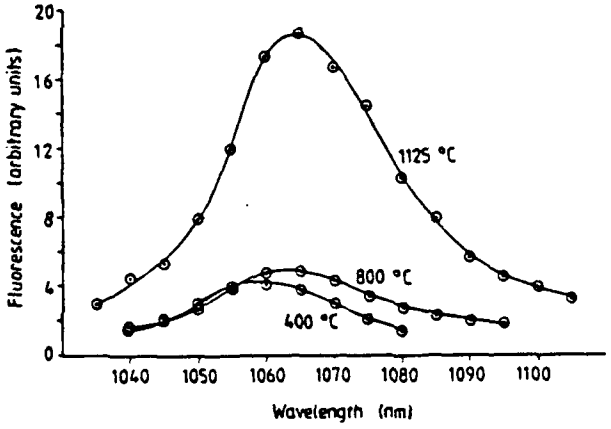

Figure 2. Fluorescence intensity against wavelength for 5 wt% Nd_2O_3 doped gel–silica samples densified to different temperatures.

$^4F_{3/2} \rightarrow {}^4I_{9/2}$ transition. Standard laboratory spectrometers were used for absorption and FTIR measurements. Raman spectra were taken using an argon ion laser, double monochromator, cooled PMT and dedicated computer set-up.

3. Results and discussion

Initial results on samples doped only with various concentrations of neodymium gave surprisingly short lifetimes and low (qualitatively estimated) fluorescence efficiencies. Figure 1 shows the results for a batch of 5 wt% Nd_2O_3 doped samples densified to various temperatures. (Fully densified, non-porous gel–silica is obtained at a densification temperature of ~1200 °C.) Note that all the lifetimes are less than 10 μs, in stark contrast to expected values of 200–800 μs (Yariv 1976). Figure 2, however, shows that the linewidths are comparable to those for conventional laser glasses. Fuller densification appears to favour the fluorescence

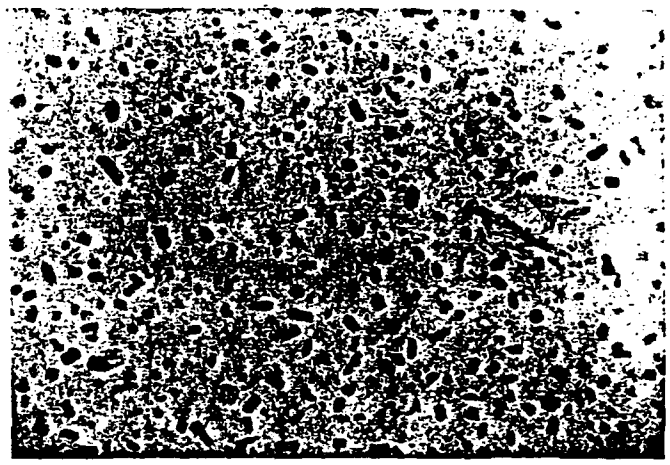

Figure 3. Transmission micrograph of a 5 wt% Nd_2O_3 doped gel–silica sample.

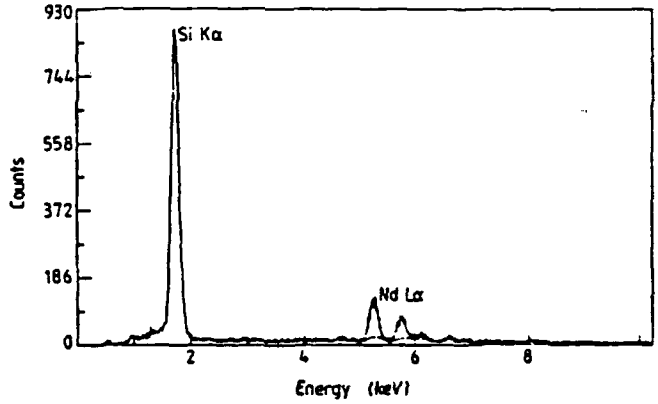

Figure 4. SEM–EDAX analysis of a 5 wt% Nd_2O_3 doped gel–silica sample from a region containing a clump (full curve) and a region not containing any clumps (broken curve).

efficiency and increase the tuning range, also shifting the peak to longer wavelengths. Similar results are obtained for the fluorescence band around 900 nm, which, since it emanates from the same $^4F_{3/2}$ lasing level, lends weight to the theory that this level is being seriously quenched. Concentration quenching is known to be a problem with Nd doping (Peterson and Bridenbaugh 1964) and clumping or clustering is known to be a problem with rare earth doping of pure silica (Arai *et al* 1986). The two effects combined could explain the short lifetimes in gel–silica samples even though their overall doping levels are below those where the effect should be observable.

Figure 3 shows a transmission micrograph of a 5 wt% Nd_2O_3 doped sample. Clumps with dimensions of the order of 100 nm are clearly visible. A greater magnification still shows structure within a single clump and electron diffraction traces show rings, again indicative of structure within the clumps. That all the neodymium is contained within the clumps is confirmed by SEM–EDAX measurements performed on a region of the sample containing a clump and one without. The results are shown in figure 4 and reveal an Nd signal from the clump-containing region only.

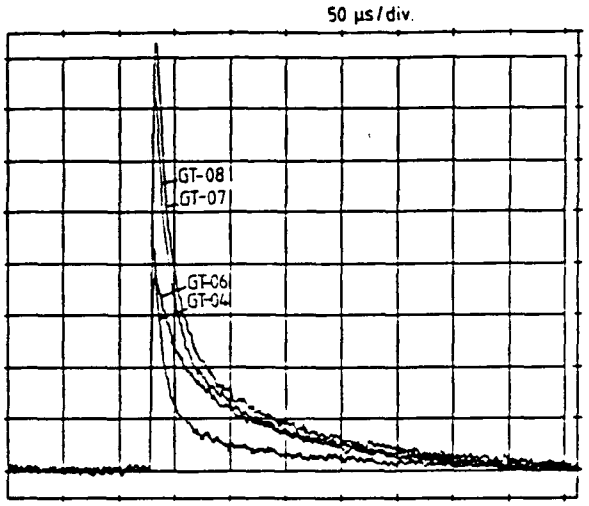

Figure 5. Temporal profiles of the 1.06 μm fluorescence from various gel–silica samples co-doped with Nd and Al.

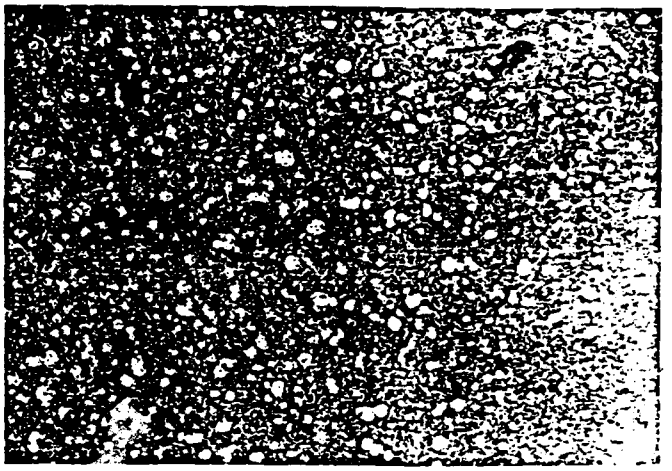

Figure 6. Transmission micrograph of the co-doped sample GT-06.

Clearly the Nd ions are not being dispersed adequately throughout the gel–silica matrix. With conventional silica the solution was to co-dope with a glass modifier such as aluminium or phosphorus. Aluminium lends itself well to the sol–gel process and so the same lifetime, linewidth and fluorescence efficiency studies were performed on a new batch of samples which were co-doped with Nd and Al, the concentrations being determined by SEM–EDAX measurements.

Figure 5 shows the lifetime results for fluorescence at around 1.06 μm. The concentrations of dopants were (wt% of oxides); GT-04 (3.5% Nd:5.0% Al), GT-06 (1.5% Nd:7.0% Al), GT-07 (3.5% Nd:7.4% Al) and GT-08 (4.6% Nd:7.1% Al). The lifetimes are now much longer, although the temporal profiles appear to consist of the same initial rapid decay seen in the samples doped only with Nd followed by a more long-lived decay. This is except for sample GT-06 which does not appear to have the initial decay, and has, in fact, got a longer final decay than the other samples (>100 μs). Note also that this sample has the highest Al/Nd dopant ratio of those shown, these results and others indicating that a dopant ratio Al/Nd ≥ 5 is required. A similar result was obtained by Arai *et al* (1986) for the co-doping of conventional silica. It appears, therefore, that co-doping with a glass modifier can overcome the clumping and consequent concentration quenching problem in sol–gel derived silica. This result is verified by the fact that fluorescence efficiencies are greatly improved. Conclusive proof is given, however, by the transmission micrographs of sample GT-06 shown in figure 6. The clumps (dark patches in figure 3) have clearly disappeared, being replaced, in this case, by white patches. These patches represent holes in the matrix caused by bloating in the as yet unperfected densification process for co-doped samples. SEM–EDAX measurements performed anywhere on the sample give the same Nd signal, a result again indicative of good dispersion throughout the matrix.

Although much improved, however, the linewidths are still not as long as expected and the fluorescence efficiencies are still not as high as those for samples of conventional silicate laser glasses. (The linewidths are, however, comparable.) An additional quenching process is suspected, the nature of the sol–gel process leading credence to the theory that phonon quenching due to residual OH^- ion content is a likely candidate. This has been identified as a problem in other laser glasses by, for example, Bondarenko *et al* (1976), where the effect can be quite large. As an example, Bondarenko *et al* derive an equation for a phosphate glass

$$1/\tau = 3.3 \times 10^3 + 2.2 \times 10^2 \sigma$$

where τ is the upper lasing level lifetime and σ (cm^{-1}) is the absorption coefficient at 2.85 μm (i.e. the fundamental absorption band of OH). If our sol–gel derived silicate glasses are anything like this example then the lifetime is being reduced if the transmission through a typical 5 mm thick sample falls below ~50% at 2.85 μm. Incomplete densification and an unperfected dehydration technique for co-doped samples results in a large residual OH^- ion content, as the absorption profiles of figure 7 reveal for the GT series of co-doped samples. None of these samples reveal any transmission at all at 2.85 μm, and so some quenching effect is not unexpected. Complete removal of OH^- ions would mean, for example, that the trace for GT-04 would be level right out to 3300 nm, showing no troughs at the OH absorptions of about 2700, 2200, 1900 and 1380 nm. This has been achieved for undoped sol–gel derived silicas, but the presence of dopants makes the process more difficult. Another manifestation of this difficulty is the falling off in the transmission of some of the samples in figure 7 as one goes to shorter wavelengths. This is caused by scattering from the small voids in the matrix caused by bloating during the densification process, an effect which also gives the samples a slight milky appearance.

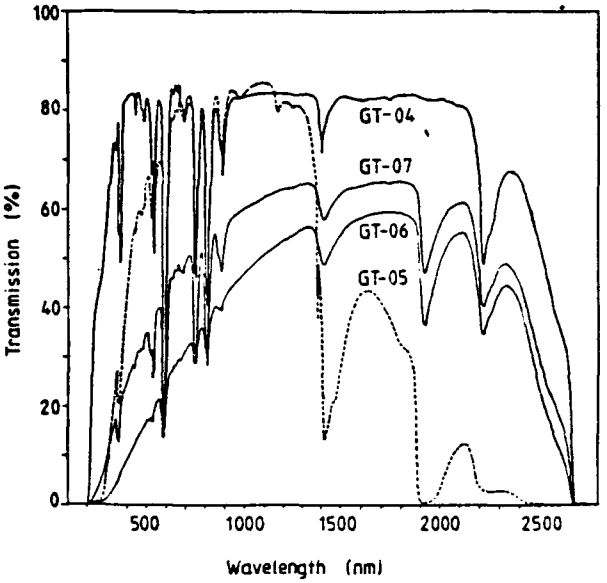

Figure 7. Absorption spectrometry traces of various gel–silica samples co-doped with Nd and Al.

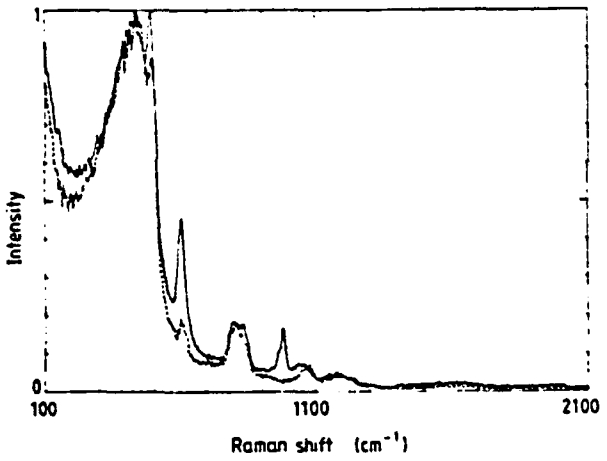

Figure 8. Raman spectra of partially densified undoped gel–silica (full curve) and fully densified and dehydrolysed undoped gel–silica (broken curve).

FTIR spectroscopy, scanning the wavelength range 2.5–25 μm, also reveals the 'wetness' of all the doped samples tested to date, as does Raman spectroscopy. Using the experimental arrangement already described, Raman spectra such as those shown in figure 8 are obtained for an undoped, partially densified sample and an undoped, fully densified and dehydrated sample. These spectra are essentially the same as those obtained by Stolen and Walrafen (1976) for conventionally produced silica. Particular points to note are the peak at about 970 cm^{-1} in the partially densified sample—a peak which Stolen and Walrafen attribute to the Si-(OH) vibration—and the relatively larger sizes of the defect peaks at about 490 and 604 cm^{-1}, again in the partially densified sample. Raman spectra from all the co-doped samples show various levels of fluorescence signal which either totally or partially obscure the Raman signal, the effect appearing to be in proportion to the visual milkiness of the sample. The samples that gave traces most like those of figure 7 were two with Al/Nd ≥ 5, the defect peaks not being present and fluorescence only starting at shifts greater than about 1100 cm^{-1}. Although little understood as yet, it is clear that Raman spectroscopy is a powerful tool in the investigation of the microstructure of doped sol–gel derived silica matrices.

4. Conclusions

Initial measurements of the fluorescence lifetime of the $^4F_{3/2} \rightarrow {}^4I_{11/2}$ transition of Nd doped into sol–gel derived silica found it to be too short and the fluorescence efficiency much too low. Both these effects suggested concentration quenching. TEM measurements revealed the expected clumping of the Nd_2O_3 and we have shown that co-doping with a glass modifier such as Al prevents this effect provided the dopant ratio Al/Nd ≥ 5. We show, however, that the samples available to date are still too 'wet', residual OH^- ions probably being responsible for the still lower than expected lifetimes and fluorescence efficiencies that we are observing. OH^- can be successfully removed in undoped samples, however, and Geltech Inc. are confident that the same will also apply to co-doped samples. When this has been achieved, and high-optical-quality rod-shaped samples have been manufactured, it will only be a matter of time before successful lasing action, with limited tunability, can be reported for the first time in a rare-earth doped sol–gel derived silica host.

Acknowledgments

This study forms part of a wider programme of research in collaboration with the Advanced Materials Research Center, University of Florida and Geltech Inc. We have enjoyed extensive discussions with Professor Larry Hench of the AMRC and we thank Mr Bill Moreshead of Geltech Inc. for discussion and provision of samples. This research has been sponsored by the Air Force Office of Scientific Research (AFSC) under contract F49620-88-C-0010.

References

Arai K, Namikawa H, Kumata K, Honda T, Ishii Y and Handa T 1986 *J. Appl. Phys.* **59** 3430

Bondarenko E G, Galant E I, Lunter S G, Przhevaskii A K and Tolstoi M N 1976 *Sov. J. Opt. Technol.* **42** 333

Levine A K 1968 in *Lasers* vol 2 (London: Edward Arnold)

Peterson G F and Bridenbaugh P M 1964 *J. Opt. Soc. Am.* **54** 644

Stolen R H and Walrafen G E 1976 *J. Chem. Phys.* **64** 2623

Yariv A 1976 *Introduction to Optical Electronics* 2nd edn (New York: Holt, Rinehart and Winston)

APPENDIX D

DOPED GEL-SILICA LASER HOSTS

T.A. King, D. Shaw, C. Whitehurst
Physics Department, Manchester University
Manchester M13 9PL

1. Rare Earth Doping of Gel-silica

Work has initially concentrated on the doping of gel-silica hosts with neodymium because of its well-known lasing properties. Investigations have concentrated on measuring various laser relevant properties such as; fluorescence lifetimes, fluorescence bandwidths, fluorescence efficiencies, dopant dispersion throughout the medium, absorption spectra and optical quality. The salient results obtained to date are as follows;

(a) Initial samples doped with various concentrations of Nd only (0.5-5wt% oxide) revealed anomalously short lifetimes ($<10\mu s$)(fig.1) and poor efficiencies. Bandwidths were acceptable, however, showing potential for limited tunability.

(b) TEM micrographs showed clumps. SEM-EDAX measurements revealed that the neodymium was in the clumps (fig.2) and not in the matrix between them. This clumping, and resultant concentration quenching, would account for the short lifetimes and poor efficiencies.

(c) Co-doping with Al (a glass modifier amenable to the sol-gel process) appears to aid Nd dispersion throughout the medium. A ratio Al/Nd$\geq$4.5 seems to result in longer lifetimes ($>100\mu s$)(fig.3, sample GT-06), the TEM micrograph showing no clumping and the SEM-EDAX measurements being the same from any region of the sample taken at random. The bandwidths remain unchanged.

(d) Fluorescence efficiencies are still low compared with a sample of typical silicate glass. Linewidths are still shorter than expected. Residual OH^- ion concentration is suspected of being responsible for phonon quenching. Figure 4 reveals that all co-doped samples to date are "wet" (ie. large absorption at eg. $2.85\mu m$). FTIR and Raman spectroscopy reveal the same thing, the latter technique, however, showing considerable promise as a diagnostic tool in the investigation of the doped sol-gel microstructure.

Some rod-shaped samples were obtained and the apparatus constructed for gain measurements and an attempt at lasing. The samples were of poor quality, however, and no gain could be measured. The apparatus is now in place, however, for any future attempts with better samples. High quality, dry, undoped samples can be made and we are optimistic that if the densification process can be perfected for co-doped rod-shaped samples then an operating rare earth doped sol-gel derived glass laser will soon be demonstrated.

APPENDIX E

Journal of Non-Crystalline Solids 121 (1990) 136–142
North-Holland

POROUS GEL–SILICA, A MATRIX FOR OPTICALLY ACTIVE COMPONENTS

Jean-Luc R. NOGUÈS and William V. MORESHEAD
Geltech, Inc., One Progress Boulevard, Box 18, Alachua, FL 32615, USA

The sol–gel process has been used to prepare optically active components in a silica matrix. In most cases this involves introducing an optically active material such as an organic dye into the initial sol prior to gelation. An alternative sol–gel route involves first the preparation of porous, pure silica monoliths which can then be impregnated with the desired organic or inorganic material. Critical to the usefulness of this material is a knowledge of the properties, such as thermal stability, UV/vis/nIR spectra and pore size. The structural evolution of these porous silica monoliths prepared by the sol–gel process is presented as a function of process temperature. Sample preparation and thermal treatments are briefly described, and results of sample characterizations are given in detail. Results of this study and their implications for the usefulness of the materials are discussed.

1. Introduction

Over the past several years there has been an increasing interest in sol–gel techniques for the manufacture of glasses, glass-ceramics and ceramics. This new route has been utilized for a variety of products ranging from optical fibers and lenses to special coatings and to production of ultra-pure powders. As early as 1984, organic molecules were added to monoliths prior to gelation [1,2], porous thin films [3] and more recently partially densified monoliths [4].

The purpose of this paper is to focus in a first part on the processing and the properties of porous gel–silica glass monoliths to be used as a matrix for the preparation of optically active components and new kinds of optical devices. This new material presents many properties of the dense pure silica glass but presents in addition many unique characteristics which could lead to very special and novel developments in optics. Several applications such as micro-optical arrays, scintillation detectors and optical waveguides are briefly described in the second part of this paper.

2. Porous gel–silica matrix preparation, processing, and properties

2.1. Experimental

The porous gel–silica samples used in this study were manufactured by hydrolyzing a silica precursor, tetramethylorthosilicate (TMOS, Hüls America Inc.) with deionized water. After complete homogenization this sol was cast into 60 mm polystyrene petri dishes to gel and age. The wet gel was then dried to give a transparent gel–silica monolith.

Further heat treatment was done in static air to study the evolution in gel properties with temperature. The rate of heating was sufficiently small to maintain the monolithic aspect of the gels and to avoid a temperature gradient inside a sample which can cause heterogeneity in gel properties. Isotherms at 620 and 800 °C were measured to evacuate solvent and by-products from the gel structure, and to observe the evolution in sample properties during a soak. Samples were removed from the furnace at a given temperature and

0022-3093/90/$03.50

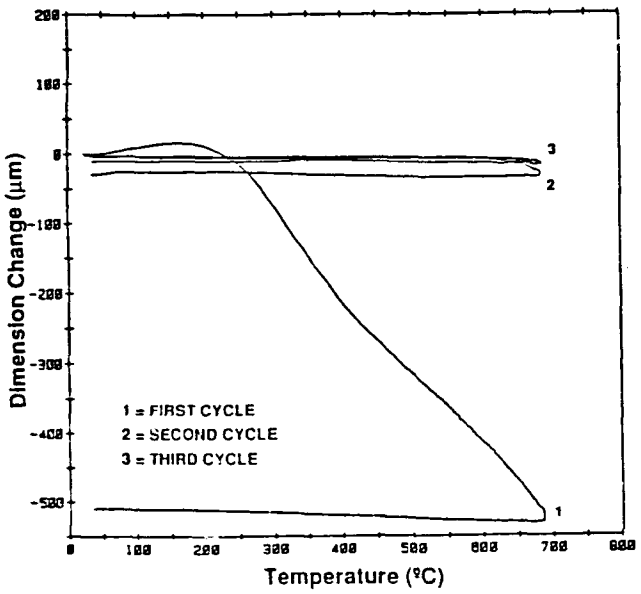

Fig. 1. Thermomechanical analysis of a porous gel-silica monolith.

quenched in air at room temperature. Shrinkage during densification was measured in static air using a Dupont 943 Thermomechanical analyzer (TMA). The heating rate was 0.5 °C/min.

The textural characteristics were measured using an Autosorb-6 from the Quantachrome Corporation. The results were analyzed according to the BET theory and a cylindrical pore model was used for the calculations of the pore radius distribution. The density measurements were carried out on oven-dried samples using a specific gravity bottle with mercury as the fluid. The microhardness was measured using a LECO Model-700 Microhardness Tester with a diamond Vickers indenter. UV-vis-nIR spectra were recorded on a Lambda-9 Spectrophotometer from Perkin-Elmer.

2.2. Results and discussion

Figure 1 presents the TMA thermogram of a dry gel monolith between room temperature and 685 °C, the maximum temperature of the equipment. The heat treatment cycle was repeated three times without removing the sample from the cell, and with recalibration of the zero position before each cycle.

After the first cycle to 685 °C the sample underwent a net shrinkage of 8.4% after returning to room temperature. After the second cycle the shrinkage was not negligible but was greatly reduced (0.5%). A third cycle resulted in an additional shrinkage of 0.2%.

These results lead to an important conclusion regarding the usefulness of these materials as porous matrices: further heating to a temperature close to, equal to, or higher than the maximum

Table 1
Properties and characteristics of porous gel-silica monoliths versus densification temperature

Temperature (°C)	SSA (m^3/g)	TPV (cm^3/g)	APR (Å)	SBD (g/cm^3)	SMH (kg/m^3)	[OH] (a.u.)
200	768	0.47	12.2	1.172	41	193
400	707	0.42	11.8	1.224	65	189
550	672	0.39	11.7	1.299	88	172
620	620	0.37	11.8	1.308	101	161
620	537	0.31	11.6	1.391	97	157
700	522	0.30	11.6	1.393	115	143
750	449	0.26	11.7	1.424	160	132
800	438	0.26	11.8	1.438	183	122
800	393	0.23	11.7	1.460	-	122
850	-	-	-	1.502	233	94
900	290	0.17	11.8	1.510	285	66
950	9	0.01	13.9	2.113	447	9
1000	4	0.00	15.6	2.109	-	-
1050	3	0.00	16.8	1.651	-	-

SSA: specific surface area; TPV: total pore volume; APR: average pore radius; SBD: sample bulk density; SMH: sample microhardness; [OH]: OH radical content.

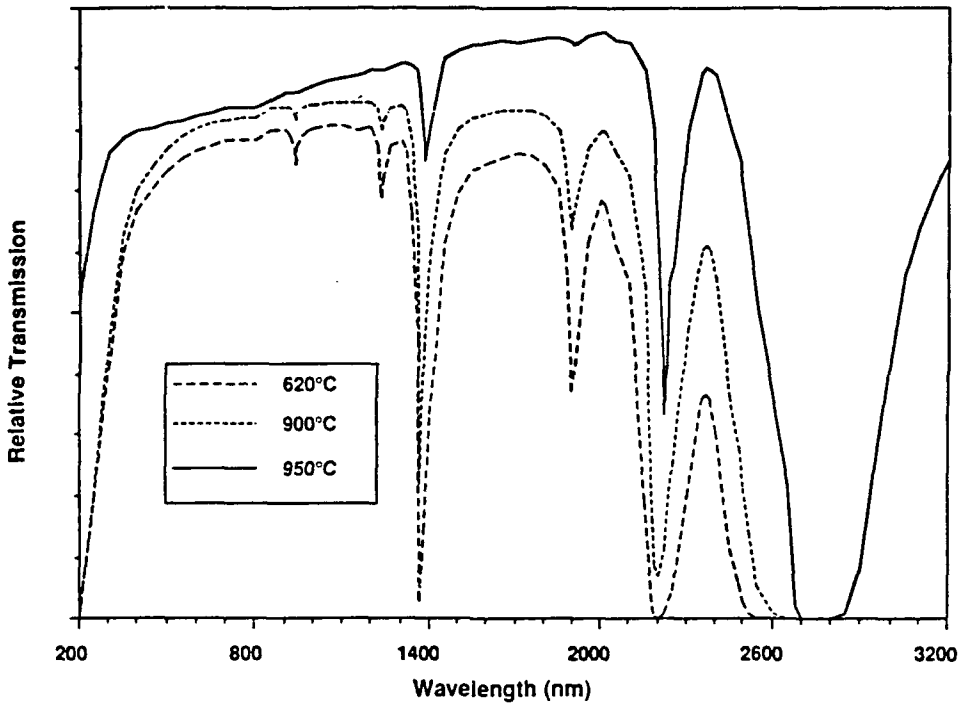

Fig. 2. Optical transmission of gel-silica monolith versus densification temperature.

temperature to which the gel has been previously heated will induce new variations in the structure of the gel-silica. However, a sample can be considered to be thermally stable at temperatures well below this maximum temperature.

Changes in other gel characteristics and proper-

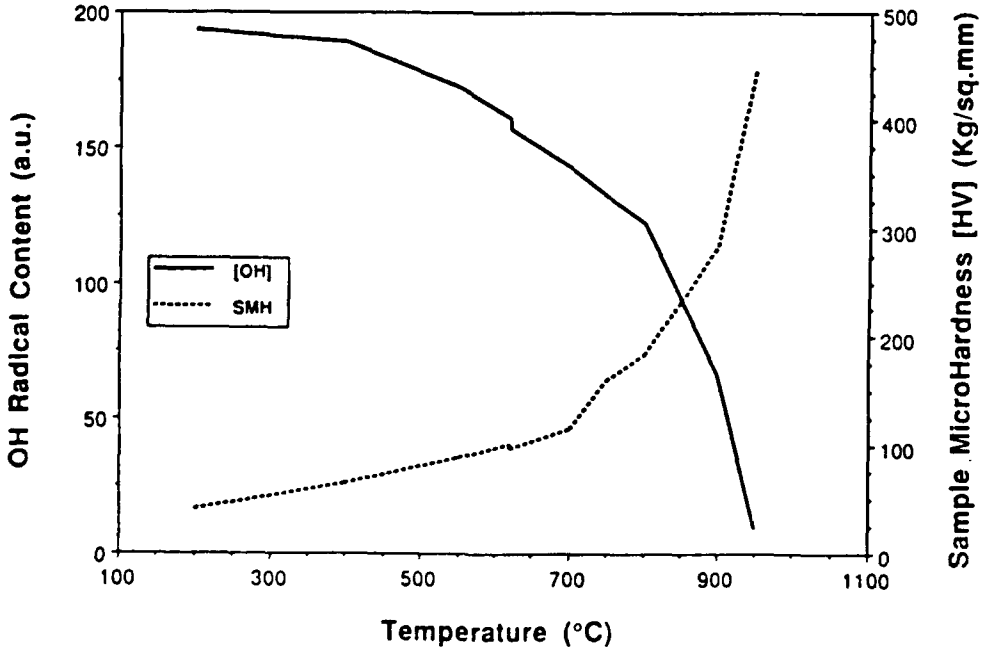

Fig. 3. OH radical content ([OH]) and sample microhardness (SMH) versus densification temperature.

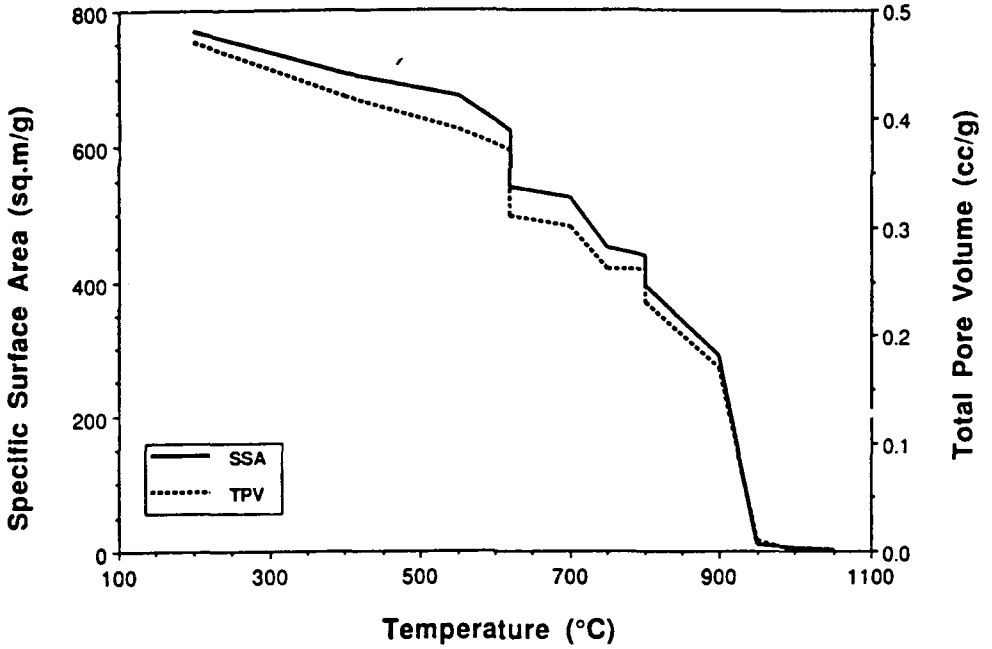

Fig. 4. Specific surface area (SSA) and total pore volume (TPV) versus densification temperature.

ties measured for this study during densification are in good agreement. The results are summarized in table 1. These changes are smooth and regular as the treatment temperature is increased to 950 °C. At this temperature the properties of the gel change drastically and the material loses characteristics suitable for porous matrix applications. Although the magnitude of the changes are greater for the soak at 620 °C than for the soak at 800 °C, the trends were similar.

The transmission spectra of samples stabilized at 620, 900 and 950 °C show the well-known absorption bands due to silanol groups (Si–OH) and molecular water (fig. 2) [5–7]. With the stabilization temperature increasing, two phenomena occur: (1) the absorption bands decrease in intensity corresponding to the release of 'water' by the sample, and (2) the transmission cutoff in the ultraviolet range shifts to lower wavelengths. For the sample stabilized at 950 °C the spectrum presents only the major absorption bands of Si–OH.

Figure 3 shows the variation of OH radical concentration in the gel as a function of temperature. The calculation of this OH radical content was done using a formula derived from the one used for OH content determination in silica glasses [8] and applied to the absorption band at 1.36 μm of the first overtone of the fundamental absorption peak of Si–OH groups (2.73 μm). Since the extinction coefficient is not presently available to quantify the water content using this band, the results are plotted in arbitrary units. However, this figure shows that the OH radical content in the gel decreases rapidly with increasing temperature.

The data collected in this study allow the definition of three different sequences during the sintering treatment.

(1) Between room temperature and 900 °C there is a continuous evolution of gel properties. This evolution is faster for the higher temperatures, especially between 800 and 900 °C. This evolution occurs mainly by loss of water. The specific surface area and the total pore volume decrease as a result of condensation reactions which cause the network to become more and more interconnected without causing any change in the calculated average pore radius (fig. 4). As interconnectivity increases the bulk density and microhardness increase by the same trend, as expected (table 1). The trend in microhardness is illustrated in fig. 3.

(2) Between 900 and 950 °C the densification

takes place more rapidly since the viscosity of the material is low enough to allow viscous sintering. Measured changes are much more dramatic.

(3) Above 950 °C, pores remaining in the sample begin to close resulting in bloating of the sample. At this stage the sample loses its transparency, its homogeneity and its ability to be used as a porous matrix for optical components.

The ultrastructure data also show that the sintering of this particular type of gel silica occurs without variation of the average pore size, maintaining or enhancing the optical transmission of the porous sample.

3. Potential applications of porous gel-silica matrices

The properties and characteristics of porous gel-silica, in particular porosity and transmission, make this material adequate for the development of new types of optical elements [9]. The porous phase of this gel-silica matrix can be filled with a second phase with very special properties to produce a composite material. The completely open porosity and the very small size of the pores allow the production of a nanoscale composite with good macro-homogeneity. The doping phase can be either an inorganic material such as metallic cations or an organic compound which leads to the preparation of organic/inorganic composites. Examples of these two types of applications are briefly described below, as well as a possible direct application of the porous gel-silica matrix.

3.1. Micro-optical arrays [10]

The basic components for digital optics have been identified as modulator and detector arrays, which in many cases require microlens arrays for imaging. Stacked planar optics is an attractive technology for digital optics, and can be used for many possible applications, such as optical computing, camera auto focus modules, or imaging bar lenses in photocopiers.

The basic unit of the array is the individual microlens which is a region with an index gradient embedded in a glass substrate as a result of selective doping. The actual manufacture of this type of lens is difficult and often leads to optical aberrations, limiting the number of components which may be stacked together.

Sol-gel technology offers the possibility to minimize spatial aberration by doping a porous gel-silica matrix or preform. The porous gel-silica is doped selectively with polarisable ions, e.g. Ba^{2+}, or glass structure modifiers, e.g. Pb^{2+}, and the dopant elements are trapped in the glass by subsequent densification to form a microlens array.

3.2. Scintillations detectors [4]

Organic plastic scintillators have been used for particle detection for about 30 years. They have two advantages: (1) fluorescence decay times as short as 1 ns, and (2) light output proportional to energy deposition in the detector. It is well known, however, that plastic scintillators are rather sensitive to ambient radiation which results in the strong absorption of light for doses as small as 10^5 rad.

Scintillating glasses have been developed over the past 25 years but never came into general use as particle detectors. Because of the high temperature used in the production of glass, organic fluors were excluded as dopants and only inorganic dopants such as cerium and terbium oxides could be used. The advantages of scintillating glasses are that they are heavier and less sensitive to radiation than plastic scintillators. On the other hand, their fluorescence decay times have been found to be rather long.

To meet the present day rate and radiation dose requirements, it would be desirable to have a scintillator with the high radiation resistance of pure silica glass and the short fluorescence decay time of organic fluors. Because of the high radiation resistance of silica, sol-gel technology opens the exciting possibility of doping glass with fast organic fluors which would provide an important advancement in particle detection. Although the sol-gel scintillators produced to date are not optimized, the first results prove the feasibility of producing a fast, radiation hard scintillator using the sol-gel process. Reference [4] explains in de-

tail the optical characteristics of prototypes of fast, radiation hard scintillation detectors.

3.3. Optical waveguides

Optical waveguides on a glass substrate represent the basis for passive components such as multiplexers, couplers, or wavelength filters used in integrated optical applications for optical communication and sensors.

Various techniques for fabricating glass waveguides have been reported in the literature and include: techniques such as sputtering, ion implantation, ion-exchange, and chemical vapor deposition. Today, these last two techniques are the most successful. The ideal would be waveguides made in silica substrates, preferably without any dopant, for tailoring the index profile, and maintaining the monolithic nature of the devices.

The sol-gel technology leading to the manufacture of porous gel-silica matrices offers a possible substrate for waveguides. Two approaches can be pursued: first, the selective doping of the substrate using controlled diffusion in the porous silica in order to change the refractive index of the material, and second, local heating of some selected portion of the substrate to increase the density and index of refraction of the glass [11]. By CO_2 laser heating which produces densification, optical waveguides have been made using laser writing of higher density tracks on a porous gel-silica substrate [12].

It was demonstrated that both of these techniques can induce the refractive index changes of the right magnitude to fabricate single mode waveguides. The second technique presents the possibility to produce ideal pure silica waveguides. The major advantage of this type of waveguide is that it matches the index of refraction of silica fiber optics, which is not the case for ion-exchanged or diffusion based waveguides.

The technique of doping a pure gel-silica matrix with inorganic or organic compounds is not restricted to the applications described in this paper, but can be used for the preparation of a wide variety of optically active materials, such as optical filters [13], dye lasers, non linear optic components, optical data storage media, and many others.

4. Conclusion

This study showed that it is possible to produce stabilized sol-gel monoliths with a range of properties, and free of organic residues. The sintering of this type of gel silica occurs in roughly three stages, with the last resulting in pore closure and ultimate destruction of the sample above about 950 °C. If heating is stopped prior to this, a semi-stable, porous gel-silica matrix can be produced. The demonstration of possible applications of such a matrix, such as microlens arrays, scintillating detectors, and waveguides have been reported.

The authors gratefully acknowledge the financial support of Air Force Office of Scientific Research Contracts #F49620-86-C-0120 and F49620-88-C-0010 and the encouragement of D.R. Ulrich throughout this research. Also the technical assistance of Robert H. Krabill is greatly appreciated.

References

[1] D. Avnir, D. Levy and R. Reisfeld, J. Phys. Chem. 88 (1984) 5956.
[2] A. Makishima and T. Tani, Commun. Am. Ceram. Soc. 69 (1986) C72.
[3] D. Avnir, V.R. Kaufman and R. Reisfeld, J. Non-Cryst. Solids 74 (1985) 395.
[4] J.L. Noguès, S. Majewski, J.K. Walker, M. Bowen, R. Wojcik and W.V. Moreshead, J. Am. Ceram. Soc. 71 (1988) 1159.
[5] M. Grayson, ed., Encyclopedia of Glass, Ceramics, and Cement (Wiley, New York, 1985).
[6] R.F. Bartholomew, B.L. Butler, H.L. Hoover and C.K. Wu, J. Am. Ceram. Soc. 63 (1980) 481.
[7] D.L. Wood, E.M. Rabinovich, D.W. Johnson Jr., J.B. MacChesney and E.M. Vogel, J. Am. Ceram. Soc. 66 (1983) 693.
[8] J.E. Shelby, J. Vitco Jr. and R.E. Benner, Com. Am. Ceram. Soc. 65 (1982) C59.
[9] L.L. Hench, S.H. Wang and J.L. Noguès, SPIE Vol. 878 Multifunctional Materials (1988) 81.

[10] M.M. Stallard, in: Proc. US-UK Optical Glass and Macromolecular Materials Symp., Pitlochry, Scotland, 1988 (Hoechst Celanese Corporation, Somerville, NJ, 1988) p. 176.

[11] R.V. Ramaswamy, T. Chia, R. Srivastava, A. Miliou, and J. West. SPIE Vol. 878 Multifunctional Materials (1988) 86.

[12] D.J. Shaw, A.J. Berry and T.A. King, in: Proc. US-UK Optical Glass and Macromolecular Materials Symp., Pitlochry, Scotland, 1988 (Hoechst Celanese Corporation, Somerville, NJ, 1988) p. 13.

[13] S.H. Wang and L.L. Hench, in: Science of Ceramic Chemical Processing, ed. L.L. Hench and D.R. Ulrich (Wiley, New York, 1986) p. 201.

APPENDIX F

LASER DEVELOPMENTS IN SOL-GEL GLASS

D.Shaw, C.Whitehurst, A.Charlton and T.A.King.

Physics Department

Schuster Laboratory

University of Manchester

Manchester

M13 9PL.

TUNABLE SOLID STATE GLASS LASERS.

Introduction

A new type of laser based on a doped sol-gel glass host has recently emerged. The sol-gel glass can either be doped with inorganic ions in the fully densified state or with organic molecules in the partially densified state. Inorganically doped sol-gel holds certain advantages over traditional materials by providing a high purity medium, high power operation, low non-linear refractive index (n2) and a constant and very low coefficient of thermal expansion.

Organically doped sol-gel provides an enhancement of the laser properties of organic dyes. This involves: molecular immobility / isolation which reduces collisional deactivation; greater heat dissipation (thermal conductivity of sol-gel = 1.3 $Wm^{-1}k^{-1}$ c.f. methanol 0.2 $Wm^{-1}k^{-1}$) which reduces thermal lensing and enables higher power densities to be attained; increased dye photostability and upper state lifetime; reduced dimerisation and thus reduced self quenching and absorption; and a greater dye concentration for a more compact and efficient cavity design. Finally, a departure from the traditional liquid state for the dye medium will lead to a more convenient and manageable glass state.

Results

1. Inorganic: Uniform Nd^{3+} ion distributions were produced by the use of an Al glass modifier. Characterisation of the doped glass was performed by TEM, SEM-EDAX and Raman spectroscopy. The Nd^{3+} fluorescence lifetimes and efficiencies have been measured and for deuterated samples are now found to be comparable to other laser glasses (figure 5), indicating that phonon quenching of the upper laser state by hydroxyls is no longer a problem. Therefore the Nd^{3+} exists in the host in a form suitable for laser action.

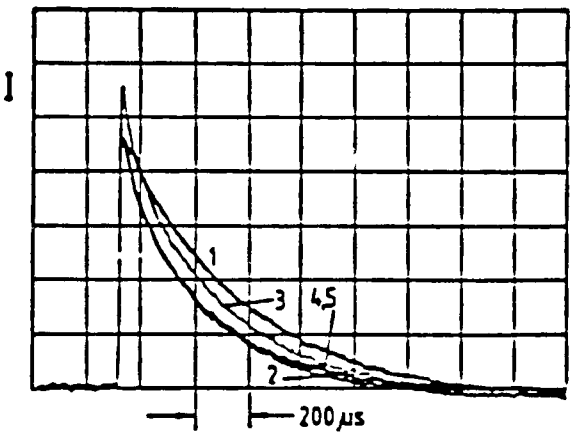

Figure 5.
Lifetimes of Nd^{3+} in laser glass (1,2) and in sol-gel glass (3,4,5)

2. Organic: Successful laser systems have been demonstrated with Rhodamine 6G doping of partially densified (850^{0}C) sol-gel glass (figure 6). Laser action was observed both with excimer laser pumping and flashlamp pumped dye laser pumping with pulse durations of 10ns and 2μs respectively. The emission spectra and temporal profiles showing the spontaneous emission and laser output when pumped by the flashlamp pumped dye laser are shown in figure 7. In this case the doped sol-gel laser, for heavy duty pumping (0.2J/mm^3) had a lifetime of approximately 10 laser shots.

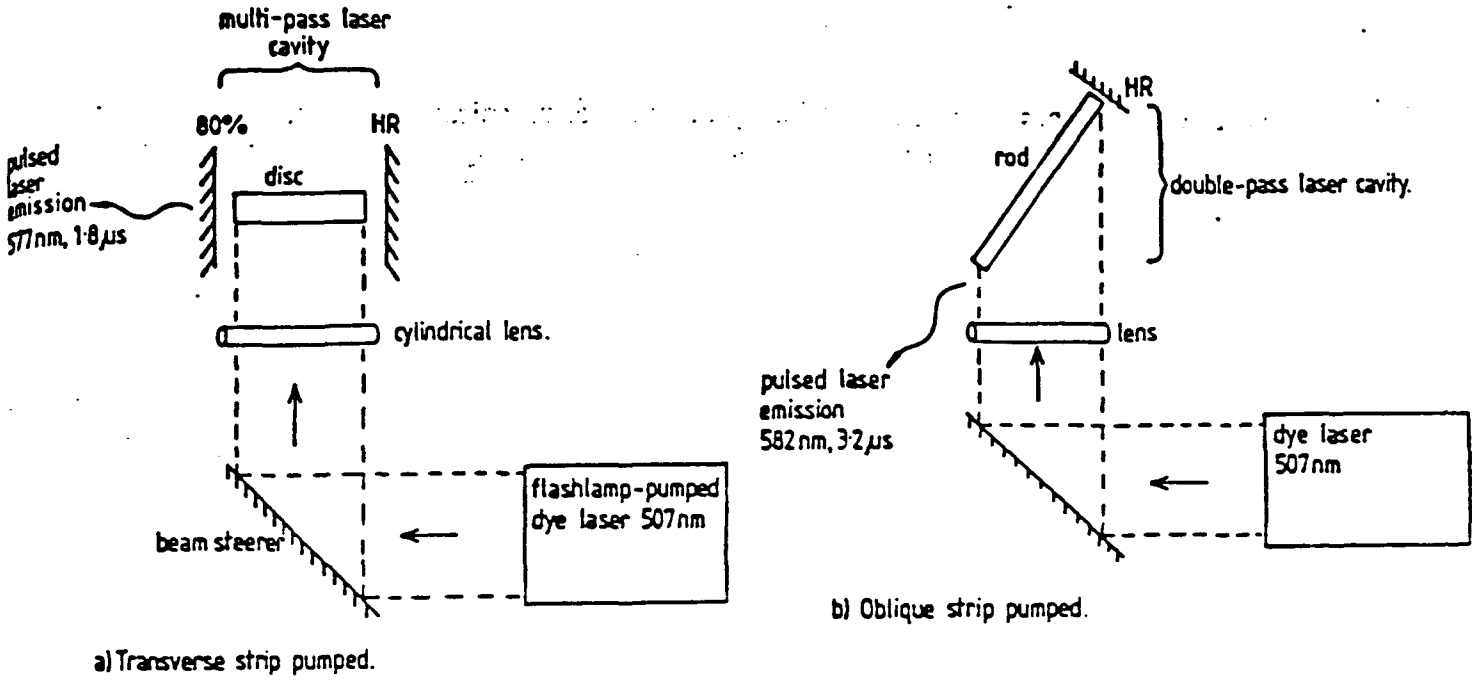

Figure 6.
Arrangements for laser pumping of organically doped sol-gel samples

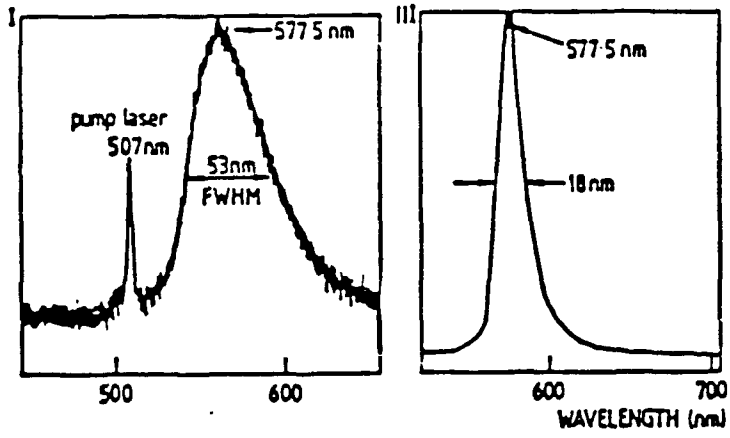

SPECTRAL PROFILE

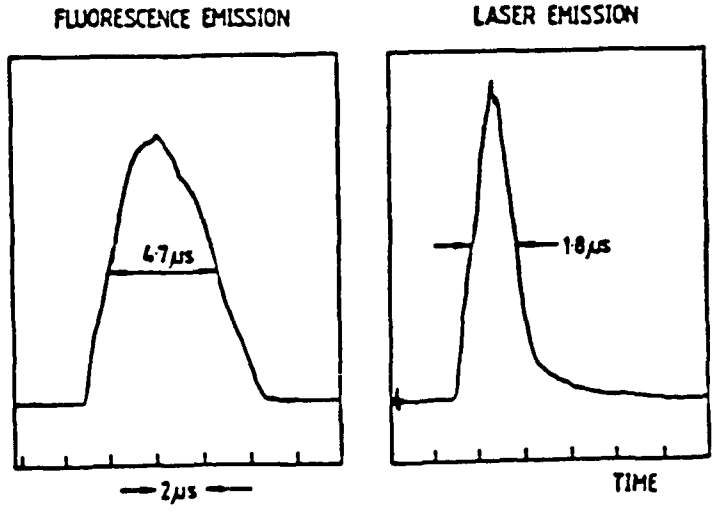

TEMPORAL PROFILE

Figure 7.
Spectral and temporal profiles showing laser output from organically doped sol-gel sample.